

**SEPARATION OF METALLIC AND SEMICONDUCTING SINGLE
WALLED CARBON NANOTUBES USING AQUEOUS TWO-
PHASE TECHNIQUE**

MALCOLM TANG SIONG YII

**DISSERTATION SUBMITTED IN FULFILLMENT OF
THE REQUIREMENT FOR THE DEGREE OF
MASTER OF SCIENCE**

**DEPARTMENT OF PHYSICS
FACULTY OF SCIENCE
UNIVERSITY OF MALAYA
KUALA LUMPUR**

2014

UNIVERSITI MALAYA
ORIGINAL LITERARY WORK DECLARATION

Name of Candidate: Malcolm Tang Siong Yii

(I.C/Passport No: 870409-52-6585)

Registration/Matric No: SGR110102

Name of Degree: Master of Science (Dissertation)

Title of Project ~~Paper/Research Report~~/Dissertation/Thesis ("this Work"):

SEPARATION OF METALLIC AND SEMICONDUCTING SINGLE WALLED CARBON NANOTUBES USING AQUEOUS TWO-PHASE TECHNIQUE

Field of Study: Nanotechnology

I do solemnly and sincerely declare that:

- (1) I am the sole author/writer of this Work;
- (2) This Work is original;
- (3) Any use of any work in which copyright exists was done by way of fair dealing and for permitted purposes and any excerpt or extract from, or reference to or reproduction of any copyright work has been disclosed expressly and sufficiently and the title of the Work and its authorship have been acknowledged in this Work;
- (4) I do not have any actual knowledge nor do I ought reasonably to know that the making of this work constitutes an infringement of any copyright work;
- (5) I hereby assign all and every rights in the copyright to this Work to the University of Malaya ("UM"), who henceforth shall be owner of the copyright in this Work and that any reproduction or use in any form or by any means whatsoever is prohibited without the written consent of UM having been first had and obtained;
- (6) I am fully aware that if in the course of making this Work I have infringed any copyright whether intentionally or otherwise, I may be subject to legal action or any other action as may be determined by UM.

Candidate's Signature:

Date: 2nd September 2013

Subscribed and solemnly declared before,

Witness's Signature:

Date: 2nd May 2014

ABSTRACT

The presence of metallic single-walled carbon nanotubes (M-SWCNT) in as-prepared single-walled carbon nanotubes (SWCNT) poses a significant hurdle to integrate carbon nanotubes into semiconductor electronics. Here the findings of enriching semiconducting single-walled carbon nanotubes (S-SWCNT) using an aqueous two-phase system (ATPS) is reported. The solution containing as received SWCNT and polyethylene glycol (PEG), dextran, *N*-methylpyrrolidone (NMP) and water effectively separates into two distinct phases, with S-SWNT dominant in one phase while the M-SWCNT congregates in another phase. The separation process is due to the attraction of amine and S-SWCNT as reported by Chattopadhyay. Micro-Raman spectroscopy and Ultraviolet-Visible spectroscopy results show evidence of the removal of M-SWCNT in one of the phases especially for volume ratio 1:1 experiment. The ratio of M_{11}/S_{22} in the top phase for V_R 1.5 reaches 0.2574 compared to 0.1507 in the bottom phase. This finding presents ATPS as an easy, effective and low-cost purification method of carbon nanotubes.

ABSTRAK

Kehadiran nanotub karbon berdinding tunggal logam (M-SWCNT) dalam sampel nanotub karbon tulen (SWCNT) merupakan satu halangan untuk mengintegrasikan nanotub karbon dalam bidang elektronik semikonduktor. Di sini penemuan dalam usaha penulenan nanotub karbon berdinding tunggal semikonduktor (S-SWCNT) dengan menggunakan sistem akues dua-fasa (ATPS) dilaporkan. Campuran yang mengandungi nanotub karbon tulen, polyethylene glycol (PEG), dextran, *N*-methylpyrrolidone (NMP) dan air didapati membahagi kepada dua fasa berbeza, di mana S-SWCNT mendominasi satu fasa sementara M-SWCNT mendominasi fasa yang satu lagi. Proses pemisahan ini adalah disebabkan kesan tarikan amine ke atas S-SWCNT seperti yang dilaporkan oleh Chattopadhyay. Spektroskopi Micro-Raman dan spektroskopi Ultraungu-Visible menunjukkan kesan pengurangan M-SWCNT dalam salah satu fasa, terutamanya untuk eksperimen bernisbah-isipadu 1:1. Nisbah M_{11}/S_{22} dalam fasa atas untuk V_R 1.5 mencapai 0.2574 berbanding 0.1507 dalam fasa bawah. Penemuan ini dapat menawarkan ATPS sebagai satu teknik penulenan yang mudah, berkesan dan berkos rendah.

ACKNOWLEDGEMENTS

I wish to express my greatest gratitude and appreciation to my supervisor, Dr. Woon Kai Lin for his kind supervision and guidance throughout the course of the study. His expertise in carbon nanotube-based materials has been a great help in my work.

My sincere gratitude also goes to my co-supervisor, Prof. Dr. Ling Tau Chuan. His support and encouragement have been very helpful during difficult times. His experience and patience helped me to overcome technical difficulties during the course of my work.

I would also like to express my sincere thanks to my colleague, Assoc. Prof. Show Pau Loke (University of Nottingham, Semenyih), Ling Yew Kiat, Chua Chong Lim and Yeoh Keat Hoe for their help and time spent for discussion. Without their tireless explanation and help, it would be impossible for me to accomplish the objective of my work.

I would like also to thank University of Malaya for the University of Malaya Fellowship Scheme (SBUM) and Postgraduate Research Fund (PPP).

Last but not least, I would like to extend my appreciation to my family members back in my home state of Sarawak. I would certainly not have been able to complete this project without their support.

LIST OF PUBLICATIONS

Manuscript type: Journal article (ISI-cited)

1.

Malcolm S.Y. Tang, T. J. Whitcher, K.H. Yeoh, C.L. Chua, K.L. Woon, P.L. Show, Y.K. Lin, T.C. Ling

The removal of metallic single-walled carbon nanotubes using an aqueous two-phase system. Journal of Nanoscience and Nanotechnology, 2014, 14(5), 3398-3402

2.

Malcolm S.Y. Tang, Pau Loke Show, Yu Kiat Lin, Kai Lin Woon, Chin Ping Tan, Tau Chuan Ling

Separation of single-walled carbon nanotubes using aqueous two-phase system, Separation and Purification Technology, 2014 (125), 136-141

Patent

1.

SEPARATION OF SEMICONDUCTING SINGLE-WALLED CARBON NANOTUBES
AND METALLIC SINGLE-WALLED CARBON NANOTUBES

PI: 2014700272

Conference

1.

Oral Presentation, International Conference on Solid State Science and Technology (ICSSST), 18-20 December 2012, Malacca, Malaysia.

TABLE OF CONTENTS

ORIGINAL LITERARY WORK DECLARATION	ii
ABSTRACT	iii
ABSTRAK	iv
ACKNOWLEDGEMENT	v
LIST OF PUBLICATIONS	vi
TABLE OF CONTENTS	vii
LIST OF FIGURES	x
LIST OF TABLES	xiv
LIST OF ABBREVIATIONS AND SYMBOLS	xiv
CHAPTER 1: INTRODUCTION	
1.1 Background of Research	1
1.2 Research Problems and Motivations	3
1.3 Significance and Implications of the Research	4
1.4 Overview of Thesis	4
CHAPTER 2: LITERATURE REVIEW	
2.1 Introduction	6
2.2 Carbon Nanotubes (CNT)	6
2.2.1 Growth of SWCNT	8
2.2.2 Chirality and Types of CNT	10
2.3 Aqueous Two-Phase Separation (ATPS system)	12
2.3.1 Phase Diagram	14
2.3.2 Advantages of ATPS	15
2.4 Purification of CNT	16

2.5	Purification of CNT using ATPS	19
CHAPTER 3: EXPERIMENT DETAILS		
3.1	Introduction	21
3.2	Experimental	
3.2.1	Materials	21
3.2.2	Phase Diagram	22
3.2.3	Separation Experiment	23
3.2.4	Optimization and Post Treatment	23
3.3	Characterization of Carbon Nanotubes	
3.3.1	Ultraviolet-Visible Absorption Spectroscopy	24
3.3.2	Micro-Raman Spectroscopy	27
3.3.3	X-Ray Photoelectron Spectroscopy	28
3.3.4	Fourier-Transform Infrared Spectroscopy	28
3.3.5	Atomic Force Microscopy	29
3.3.6	Field-Emission Scanning Electron Microscopy	29
3.4	Calculations and Formulae	31
CHAPTER 4: RESULTS AND DISCUSSION		
4.1	Introduction	33
4.2	Visual Analysis of ATPS—SWCNT	34
4.3	Phase Diagram	35
4.4	Optimization Table	
4.4.1	The effect of M_w on nanotubes partitioning	36
4.4.2	The effect of V_R on nanotube partitioning coefficient, purity, specific activity and purification factor	37
4.4.3	The effect of the concentration of NMP and water on V_R , K, yield, SA, PF, and purity	40

4.5	Ultraviolet-Visible Absorption Spectroscopy	42
4.6	Micro-Raman Spectroscopy	44
4.7	X-ray Photoelectron Spectroscopy Analysis	46
4.8	Fourier-Transform Infrared Spectroscopy	47
4.9	Atomic Force Microscopy	48
4.10	Field Emission Scanning Electron Microscopy	50
4.11	Mechanism	52
4.12	Effect of time, temperature and viscosity of ATPS	53
CHAPTER 5: CONCLUSION AND FUTURE WORKS		55
REFERENCES		60

LIST OF FIGURES

- Figure 1** The coordinate system on a single walled carbon nanotube: discrete model of (10,10) armchair single walled carbon nanotube of 8.147 nm length and consisting of 1340 carbon atoms arranged in hexagonal fashion, showing thickness h and radius R
- Figure 2** Transmission electron microscopy images of raw HIPCO tubes, at (a) low, and (b) high magnifications
- Figure 3** Methods of naming various types of CNT
- Figure 4** Periodic table of carbon nanotubes. The diameter of carbon nanotubes increases towards the right and down. DWNTs is the acronym for double-walled nanotubes. SWCNTs with extremely small diameter of about 0.4nm can be produced inside AFI-zeolite (microporous aluminophosphate crystallites) channels
- Figure 5** Schematic representation of a micellar system composed of surfactant, affinity ligands, and the desired biomaterial. Upon phase-separation the desired biomaterial can be concentrated in the micelle-rich phase according to affinity interactions, thereby enhancing the separation efficiency

- Figure 6** Aqueous two-phase system consisted of polyethylene glycol, polyvinylpyrrolidone, and water
- Figure 7** Schematic description of the formation of DNA-wrapped MWCNTs
- Figure 8** Functionalization possibilities for SWNTs: (a) defect-group functionalization, (b) covalent sidewall functionalization, (c) noncovalent exohedral functionalization with surfactants, (d) noncovalent exohedral functionalization with polymers, and (e) endohedral functionalization with, for example, C_{60} . For methods b-e, the tubes are drawn in idealized fashion, but defects are found in real situations
- Figure 9** A monochromatic light, I_0 , passing through a cuvette. The light intensity decreases to I after passing through the cuvette due to absorption
- Figure 10** (a) Photograph of a Hitachi SU8000 FESEM; (b) FESEM image of a polymer
- Figure 11** Photograph of an ATPS made up of PEG-NMP/dextran-CTAB system before (a) incubation, and after (b) partitioning into two distinct phases
- Figure 12** Phase diagram for PEG M_w 1500, 4000, 6000, 10000, and 20000 against dextran 40000

- Figure 13** The effect of V_R on the partition coefficient K and the purity of SWCNTs
- Figure 14** The effect of V_R on the specific activity of S-SWCNT in top and bottom phases
- Figure 15** The effect of V_R on the purification factor of all the species of SWCNT in both phases
- Figure 16** UV-Vis spectra for both top and bottom phase
- Figure 17** Baseline-subtracted spectra of the top and bottom phases from 430 nm-650 nm
- Figure 18** Raman spectra for top and bottom phases normalized at G+ peak (1581 cm^{-1}). The inset shows the RBM region of the Raman spectra. The RBM metallic peaks for the top phase are more intense compared to the bottom phase
- Figure 19** XPS of SWCNT and polymer
- Figure 20** FTIR spectra of all the constituents of the ATPS from 1800 cm^{-1} to 400 cm^{-1} (b) of NMP 50% w/w, CTAB 1% w/w, bottom phase and top phase. There is a clear indication of CTAB in the bottom phase as shown in the dashed rectangle
- Figure 21** AFM height images of SWCNT extracted from the bottom phase. Figures (a) and (b) are two different spots on a same sample. The inset of both images shows the corresponding amplitude images

- Figure 22** FESEM images of (a) polymer, (b) close-up look at the polymer, where strands of SWCNTs can be found, and (c) single strand of SWCNT
- Figure 23** Schematic representation of (a) a CTAB micelle, and (b) a reverse micelle
- Figure 24** Schematic formation mechanism of polymer around carbon nanotube sidewall in a sequence of (a), (b), (c), and (d)
- Figure 25** The vacuum filtration system that was used to wash away polymer from the carbon nanotubes
- Figure 26** The I-V test of the SWCNT-FET did not yield satisfactory results

LIST OF TABLES

- Table 1** The effect of M_w on SWCNT partitioning
- Table 2** The effect of the concentration of NMP and water on V_R , K
and yield
- Table 3** The effect of the concentration of NMP and water on the SA,
PF and purity

LIST OF ABBREVIATIONS AND SYMBOLS

A	Absorbance
ATPS	Aqueous two-phase separation
C	Carbon
CTAB	Cetyltrimethylammonium bromide
CVD	Chemical vapour deposition
FESEM	Field effect scanning electron microscopy
FET	Field Effect Transistor
FTIR	Fourier-transform infrared spectroscopy
HiPCO	High pressure carbon monoxide
I_0	Initial light intensity
I	Resultant light intensity
K	Partition coefficient
M-SWCNT	Metallic single-walled carbon nanotubes
M_w	Molecular weight
NMP	N-methylpyrrolidone
O	Oxygen
PEG	Polyethylene glycol
PEI	Polyethylenimine
P_F	Purification factor
PFO	Poly(9,9-dioctylfluorenyl-2,7-diyl)
PSS	Polystyrene sulfonate
P	Purity
SA	Specific activity

SWCNT	Single-walled carbon nanotubes
S-SWCNT	Semiconducting single-walled carbon nanotubes
TLL	Tie-line Length
T _T	Threshold temperature
UV-Vis	Ultraviolet-Visible
V _R	Volume ratio
XPS	X-ray photoelectron spectroscopy
Y _t	Yield

CHAPTER 1: INTRODUCTION

1.1 Background of Research

One of the most interesting nanomaterials found in the 21st century is the single-walled carbon nanotubes (SWCNT). Ever since its discovery by Sumio Iijima in 1992 (Iijima and Ichihashi 1993), SWCNTs have shown huge potential to be used in the electronic industry. SWCNTs are wrapped-up sheets of graphene. Graphene is a sheet of single-layered carbon atoms arranged in a two-dimensional, closely-packed honeycomb crystal lattice. The wrapping of the graphene sheet results in a one-dimensional material that is the carbon nanotubes. The thin layer of carbon atom results in high electron mobility (Durkop, *et al* 2004) as well as highly-desired mechanical (Yu, *et al* 2000) properties in carbon nanotubes. SWCNTs exhibit high length-to-diameter ratio (Wang, *et al* 2009), excellent electric (Hong and Myung 2007) and high thermal conductivity (Hone, *et al* 1999). Having high thermal conductivity also means that there is less phonon—specifically mass-defect—scattering in the tube. Ando and Nakanishi reported that the absence of backscattering is responsible for the long mean free path of SWCNTs (Ando and Nakanishi 1998).

Aqueous two phase system (ATPS) is a very useful technique for proteins purification and recovery. An ATPS is formed by dissolving the water-soluble phase components beyond a critical concentration that allows the formation of two immiscible phases (Zaslavsky 1995). It selectively partitions and concentrates target biomolecules into one of the phases. The basis of partitioning depends upon the surface properties of the particles and molecules such as size, charge, and hydrophobicity (Walter 1994). An ATPS uses water-soluble, phase separating polymer/polymer or salt/polymer system to generate a gentle purification environment that can maintain the

native structure of biomolecules (Arun 2008). An example of a polymer/salt system is polyethylene glycol (PEG)/potassium phosphate, and an example for polymer/polymer system is the PEG/dextran (Pereira, *et al* 2003). In recent years, ATPS has evolved beyond mere polymer/polymer and polymer/salt system. One example of this improvement is the alcohol/salt-based ATPS (Ooi, *et al* 2009b). Creative manipulation of ATPS such as multiple-step purification, recycling of phase components (Show, *et al* 2012a; Show, *et al* 2012b), and the introduction of aqueous two-phase flotation (ATPF) method (Bi, *et al* 2010; Li and Dong 2010) have made ATPS an even more attractive separation method. Good purification can be achieved *via* ATPS by manipulating the system properties which are involved in chemical and physical interactions of the partitioning process (Rosa, *et al* 2010). The factors that influence the outcome of separation including: type of polymer used, molecular weight (M_w) of the polymer involved (Forciniti, *et al* 1991), temperature of system (daSilva, *et al* 1997; Forciniti, *et al* 1991), pH of system (daSilva, *et al* 1997), and also the addition of salt (Zaslavsky 1995) .

Reports from literatures have shown that ATPS had been successfully used for purification of various proteins such as lipase and alcohol dehydrogenase (Madhusudhan, *et al* 2008; Ooi, *et al* 2009a). Nevertheless the use of ATPS for the purification of SWCNT has not been investigated. ATPS has a few advantages over other purification methods such as low cost, short processing time and the potential for large scale purification (da Silva, *et al* 2009).

1.2 Research Problems and Motivations

The homogeneity of as-prepared SWCNTs poses a hindrance to the integration of carbon nanotubes in the production of electronics such as transistors. An as-prepared SWCNT sample contains both semiconducting species (S-SWCNT) and metallic species (M-SWCNT) (Hong, *et al* 2011). Different species of carbon nanotubes are used for different applications. M-SWCNT is commonly used for interconnect applications or making electronic sensors (Deng, *et al* 2007) while the S-SWCNT is used to (Jimenez, *et al* 2007; Zhou, *et al* 2009) form the semiconducting channel of a field effect transistor (FET). Hence, the separation of S-SWCNT from M-SWCNT is an important step to develop high quality transistors. There are many purification methods reported by numerous authors. Some examples include microwave irradiation method (Shim, *et al* 2009), electrophoresis (Krupke, *et al* 2006; Marquardt, *et al* 2006), scotch-tape method (Hong, *et al* 2011), and DNA-assisted purification (Tu, *et al* 2009; Zheng, *et al* 2003). Method like acid treatment results in unwanted carboxylic functionalities (Hamon, *et al* 2001), while the high cost of DNA renders the DNA-assisted separation economically impractical for large scale purification. A highly cost effective purification of metallic SWCNTs is the use of combined diazonium and air-oxidation approach. One critical drawback is that the chemical reaction of SWCNTs with 4-bromobenzene diazonium takes a long period to complete. The use of microwave oven is another highly efficient and cost effective purification of M-SWCNTs. However, the thermal destruction of metallic SWCNTs using microwave induces random and uncontrollable damages to the neighbouring semiconducting SWCNTs (Shim, *et al* 2009). To date, researchers have yet to successfully find an effective, cost-efficient, scalable, and simple solution to separate the two species apart. Hence, the objective of

this work is to explore the possibility of ATPS as a purification method for separating M-SWCNTs and S-SWCNTs.

1.3 Significance and Implications of the Research

In this work, a simple and cost effective method for the separation of semiconducting SWCNTs using ATPS is reported. The enriched product will then be used to fabricate a SWCNT-FET. ATPS is chosen due to its benign nature, non-toxicity, and non-denaturing characteristics, which provides as an environmental-friendly approach. Moreover, this is also the first time that a biotechnology method is being used in the purification of carbon nanotubes, effectively integrating the two disciplines of science. Therefore, this research can provide insights into the means of controlling the purification parameters of carbon nanotubes using ATPS.

1.4 Structure of Thesis

A brief overview of the chapters in this thesis is presented as follows;

Chapter 2

Chapter 2 presents the literature review of the research. It begins with literature studies of SWCNT and ATPS. The problem of the integration of carbon nanotubes in semiconducting electronics is also discussed. Apart from that, the advantages and properties of general ATPS are also presented. Lastly, the chapter ends with the introduction of a newly-proposed ATPS to separate metallic SWCNT from a pristine carbon nanotubes sample.

Chapter 3

In chapter 3, sources of materials used in the work are introduced. Next, the construction of the phase diagram is discussed. The optimization of the new aqueous two-phase system is described. Various characterization methods involved in this research are also described in the chapter.

Chapter 4

This chapter aims to deliver the results obtained from the various analytical techniques described in the previous chapter. The effects of molecular weight and other parameters on the separation of metallic and semiconducting tubes are studied. A plausible mechanism of the separation of SWCNTs is proposed. Moreover, the effects of temperature, time, and viscosity of the ATPS on the performance of the overall separation are also discussed.

Chapter 5

This chapter concludes the entire experiment. It starts with a review on the objectives of the experiment, and ends with the suggestions for future works. The objectives are explained in accordance to the results and discussion presented in Chapter 4. Furthermore, simple and brief description about this work is made, pointing out its influence in the scientific community.

CHAPTER 2: LITERATURE REVIEW

2.1 Introduction

Nanotechnology is an area of research focused on the investigation of nano-sized materials. The word “nano” originates from a Greek word which means extremely small. Therefore nanomaterials are defined as any material with a size within in the range of 1-100 nanometers (nm). At this level, the size of atom becomes significant and several properties not seen in bulk materials can be observed. In the past, the investigation of these materials was hindered by their size. Since more sophisticated tools are being invented, we are now able to peer into the mysterious realm of nanomaterials. The progress that comes with these insights results in various applications which span across various fields namely medicine, semiconductor electronics and material sciences.

2.2 Carbon Nanotubes (CNT)

SWCNT is a one-dimensional, nano-sized cylindrical tube made up of a single or multiple sheet of honeycomb network of carbon atoms. Despite widespread assumption that CNT was discovered by Sumio Iijima in 1991, there are some factions within the scientific community who argue that the credit should go to earlier pioneers of CNT. According to an article by Monthieux and Kuznetsov published in the journal Carbon, SWCNT were formed following failed attempts to produce multi-walled carbon nanotubes (MWCNT) (Monthieux and Kuznetsov 2006). Russian scientists Radushkevich and Lukyanovich published transmission electron microscopy (TEM) images of tube-shaped, nano-sized carbon filament 41 years before the alleged

discovery by Sumio Iijima. Their publication, however, received minimal attention then due to the ongoing cold war between the Communist and Democratic bloc (Monthieux and Kuznetsov 2006). These pioneers, however, did not have the knowledge to mass-synthesize sufficient amount of CNT to study its interesting properties, which explains why they were unable to follow up with the interest in CNT.

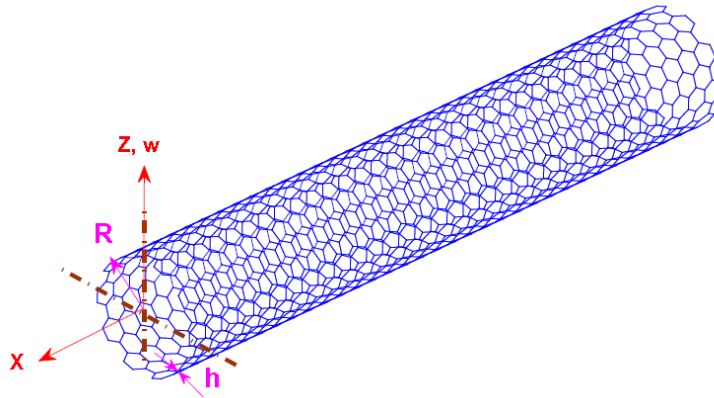


Figure 1 The coordinate system on a single walled carbon nanotube: discrete model of (10,10) armchair single walled carbon nanotube of 8.147 nm length and consisting of 1340 carbon atoms arranged in hexagonal fashion, showing thickness h and radius R (Narendar, *et al* 2012)

Iijima was working on diamond-like carbon for NEC during the 1990s when coincidentally, Donald Huffman from the United States and Wolfgang Krätschmer from Germany proposed the arc evaporation method to mass produce C_{60} , a soccer-shaped carbon molecule. Intrigued by their discovery, Iijima investigated the process for his own research. He unexpectedly found large amount of MWCNT while examining the content of a cylindrical electrode deposit produced during the arc evaporation process. His discovery was subsequently hailed as the breakthrough in nanotechnology.

2.2.1 Growth of SWCNT

There are several methods commonly used to grow carbon nanotubes. Electric arc discharge is one of the earliest methods developed to grow nanotubes. It was the method that led to the discovery of CNT by Iijima. In this method, the multi-walled tubes were found in the byproduct of fullerene production (Saito, *et al* 1992), i.e. cathode deposit, prepared by a direct current arc discharge in rarefied Helium gas (Ando 1993; Iijima 1991). By including transition metals such as iron, copper and nickel as catalysts, researchers are able to produce single-walled tubes as remnants found in the chamber soot (Bethune, *et al* 1993; Iijima and Ichihashi 1993). The resulting nanotubes are made up of tubes with various diameters and chiralities.

Apart from electric arc discharge method, the laser vaporization method is also a widely used method for producing CNT. This method was initially developed by Dr. Richard E. Smalley of Rice University, Houston to produce MWCNT (Guo, *et al* 1995a). In 1995, they used laser to vaporize the graphite-transition metal composite rod to produce single-walled tubes. The transition metals used in their method were copper and nickel. An important feature of the laser vaporization method is that it allows for continuous operation and better control over growth condition. It also produces high quality tubes in higher yield (Guo, *et al* 1995b).

Chemical vapour deposition (CVD) method for growing carbon nanotubes was developed in 1993 by José-Yacamán *et al.* (Joseyacaman, *et al* 1993). It employs the usage of transition metals—nickel, copper and iron—mixed with catalysts such as magnesium oxide, silicon dioxide and aluminium oxide in order to improve the yield (Eftekhari, *et al* 2006). These catalysts must be removed after the growth process *via* acid wash because metal catalysts can give rise to health problem (Jakubek, *et al* 2009).

Nevertheless, this method is the most suitable method for large-scale CNT production due to its relatively low unit cost.

Following the success of the CVD method, Dr. Richard Smalley's group at Rice University also developed the high pressure carbon monoxide disproportionation (HiPco) method (Bronikowski, *et al* 2001). In this method, SWNTs are produced by mixing carbon monoxide (CO) with a small amount of iron pentacarbonyl ($\text{Fe}(\text{CO})_5$) in a reactor. The thermal decomposition products react to produce iron clusters in the gas phase, which act as nuclei for SWNTs to grow. This method is able to produce up to 450 milligrams of carbon nanotubes an hour (Bronikowski, *et al* 2001).

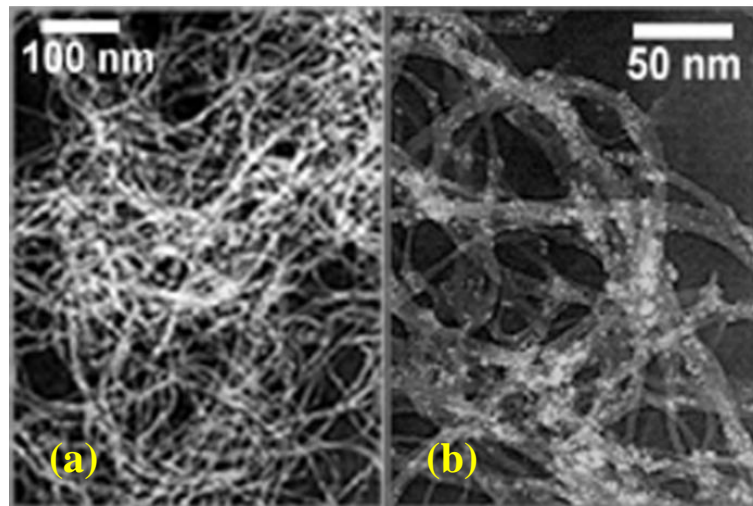


Figure 2 Transmission electron microscopy images of raw HiPco tubes, at (a) low, and (b) high magnifications (Vazquez, *et al* 2002)

2.2.2 Chirality and Types of CNT

There are several species of CNT. They are categorized by their chiral vector (n,m) , where n and m are integers of the vector equation.

$$\vec{R} = n\vec{a}_1 + m\vec{a}_2 \quad (1)$$

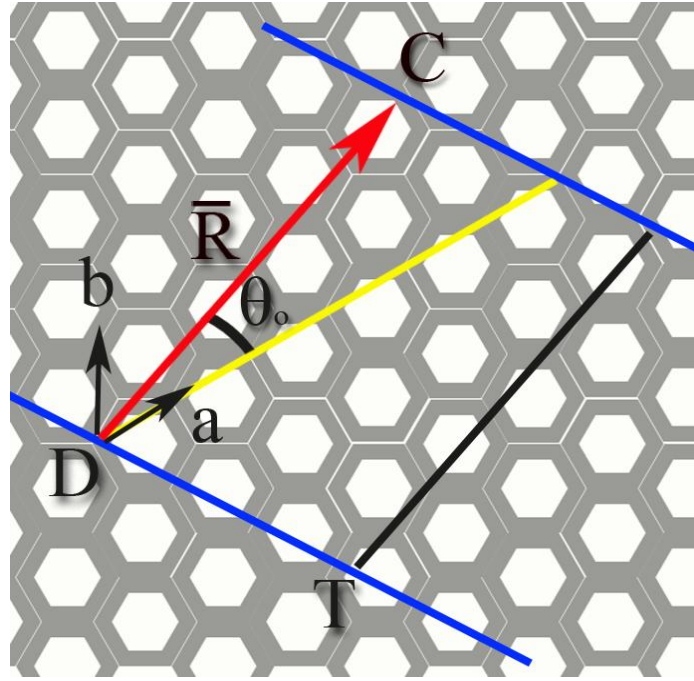


Figure 3 Methods of naming various types of CNT

To understand the concept of chiralities of CNT, one must refer to the blue and red lines in the example featured in Figure 3. Note that the two blue lines are drawn along the tube axis, with the point of intersection between the line DT and a carbon atom labelled as point D, while the point of intersection between the second tube axis and the carbon atom nearest to the armchair line is labelled as point C. An *armchair* line is represented by the yellow line. The red line, which represents the chiral vector \bar{R} , connects point C and D. The angle between the chiral vector \bar{R} and the armchair line (yellow), θ_0 decides the species of CNT. For example, the CNT is an *armchair* if the chiral vector \bar{R} falls on the *armchair* (yellow) line ($\theta_0 = 0^\circ$); if the angle $\theta_0 = 30^\circ$, the CNT is called “zigzag” nanotube; and if $0^\circ < \theta_0 < 30^\circ$, the CNT is called “chiral” tube. The diameter, d , of CNT can also be calculated *via* the equation below:

$$d = \frac{a}{\pi} (\sqrt{n^2 + nm + m^2}) \quad (2)$$

where $a = 0.246\text{nm}$, and n and m are the integers of the vector equation

Within the “chiral” family, the nanotubes are further divided into two natures—metallic and semiconducting. The tube is called metallic species M-SWCNT when the

value of $|n-m|/3$ is an integer. Therefore all *armchair* nanotubes are metallic species, but not all metallic species are *armchair* tubes. But if the value of $|n-m|/3$ is not an integer, then the CNT is called semiconducting species S-SWCNT. Different way of wrapping the graphene sheet could come up with different species of CNT, each with its own characteristic. Hence, scientists have come up with a periodic table of SWCNT to ease the recognition of different species of SWCNT (Figure 5).

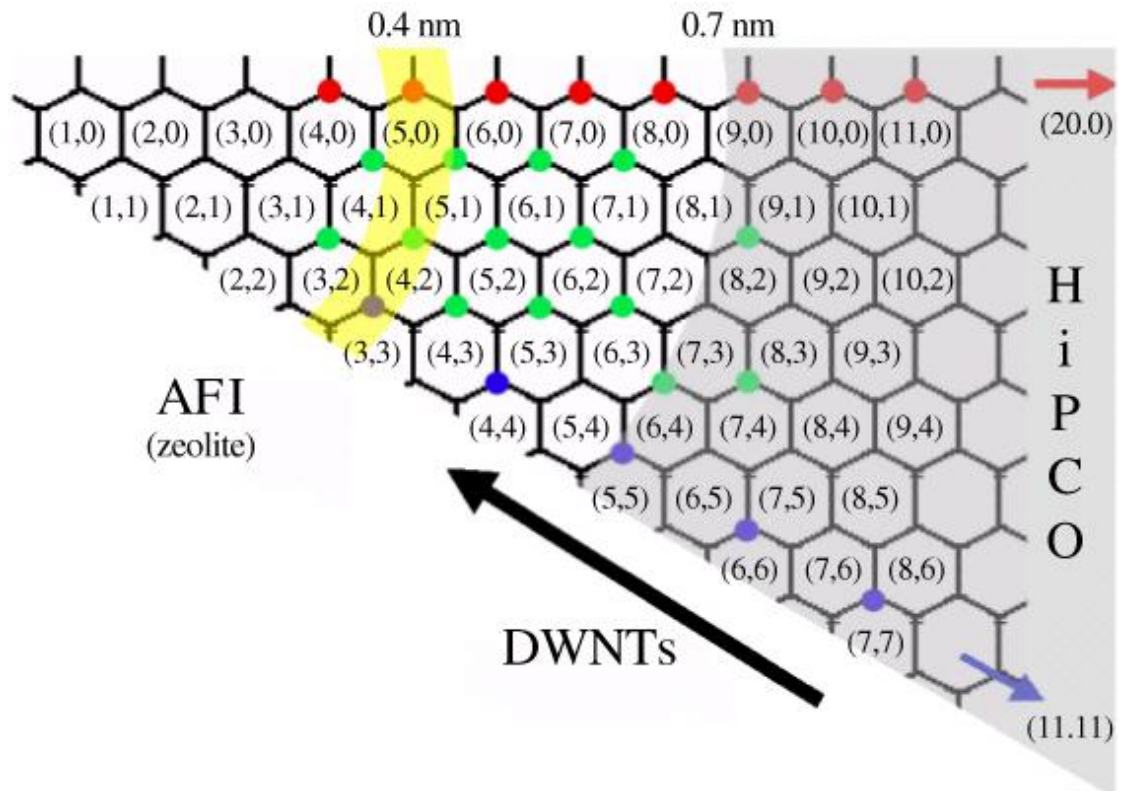


Figure 4 Periodic table of carbon nanotubes. The diameter of carbon nanotubes increases towards the right and down. DWNTs is the acronym for double-walled nanotubes. SWCNTs with extremely small diameter of about 0.4nm can be produced inside AFI-zeolite (microporous aluminophosphate crystallites) channels (Kurti, *et al* 2003; Tang, *et al* 1998)

The optical properties of carbon nanotubes are derived from the electronic transitions within their one-dimensional density of states (DOS). For semiconducting nanotubes, the valence band is separated from the conduction band by band gap E_{11} . The movement of electron across the band gap, from valance band to conduction band is known as the Van Hove optical transition, or simply denoted as S_{11} , S_{22} , etc.

Likewise for metallic species, a similar electronic transition will be labelled as M_{11} , M_{22} , etc.

2.3 Aqueous Two-Phase Separation (ATPS) system

The separation of liquid into two phases was first reported by Dutch scientist M. Beijernick (Xiao, *et al* 2000). He wrote that gelatine and agar, upon mixing beyond a certain threshold concentration, would separate into two distinct phases (Tolstoguzov 2006). 90 years later, Swedish scientist P. A. Albertsson developed the aqueous two-phase separation (ATPS) method (Albertsson 1986). ATPS has since become an efficient method for the purification of a myriad of biomaterials such as proteins, nucleic acids, virus particles, microorganism, plant and animal cells (Albertsson 1986; Hatti-Kaul 2000). A simple example of how aqueous two-phase system works is shown in Figure 5.

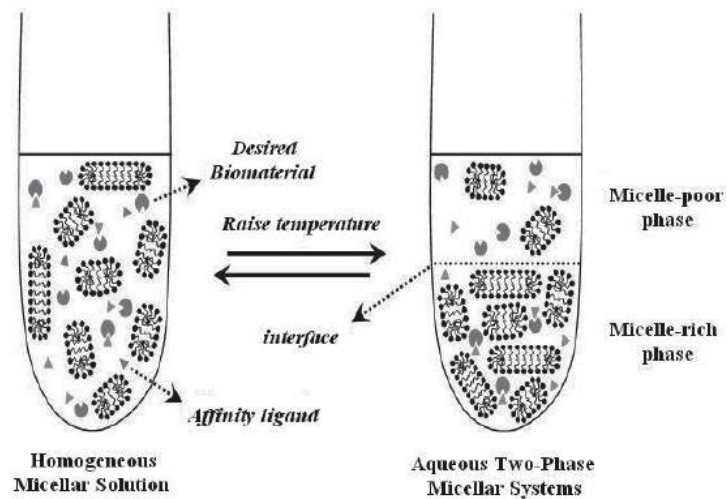


Figure 5 Schematic representation of a micellar system composed of surfactant, affinity ligands, and the desired biomaterial. Upon phase-separation the desired biomaterial can be concentrated in the micelle-rich phase according to affinity interactions, thereby enhancing the separation efficiency (Lopes, *et al* 2008)

ATPS constitutes two major procedures: equilibration and phase separation. Equilibration is a process of mixing the different phase constituents thoroughly, which involves shaking and agitation. The ATPS phase separation time needed may range from several minutes to several hours. Hence, researchers often resort to centrifugation to hasten the phase separation process (Hustedt 1985).

Mass transfer across the interface between the two phase components is possible due to the low interfacial tension of ATPS, which is only between 0.0001 and 0.1 dyne/cm (Albertsson 1986). Physical factors such as size, net charge and surface properties are the common properties that could influence the distribution of substance between the two phases. Otherwise, chemical interactions and properties such as the presence of Van der Waals' forces, hydrogen bonds, electrostatic interactions, hydrophobicity, specific affinity, and conformation effects may also affect the partitioning process (Albertsson 1986; Albertsson 1990b).

Smaller molecules are usually partitioned evenly, whereas the partitioning of larger molecules is relatively one-sided. To balance the partitioning of targeted molecules, variables such as the concentration of phase components, volume ratio (V_R), pH and the presence of additives such as salt must be optimized (Rito-Palomares 2004). An illustration of an ATPS system is shown in Figure 6.

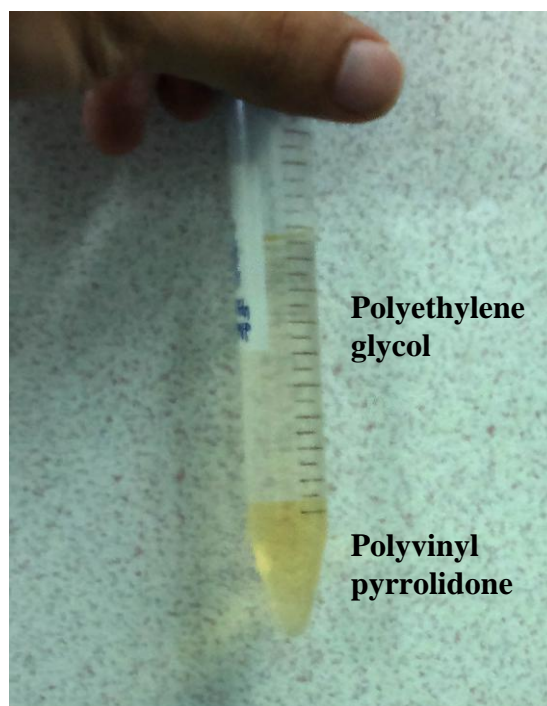


Figure 6 Aqueous two-phase system consisted of polyethylene glycol, polyvinylpyrrolidone, and water

2.3.1 Phase Diagram

A phase diagram shows the functional area of a specific ATPS. It provides information like the concentration of each component needed for the formation of two phases, the concentration of phase components in both phases, and the volume ratio (V_R) of the system (Hatti-Kaul 2000). The curve featured in the phase diagram is called binodal curve. The curve is the boundary between two-phase and single-phase region, with the region above the curve reflects the concentration of the phase-forming components required to produce a two-phase system. The common methods used to determine the binodal curve are the turbidometric titration, cloud-point method and node determination (Hatti-Kaul 2000).

2.3.2 Advantages of ATPS

ATPS is a cost efficient separation technique because it uses low cost polymers and salts, such as polyethylene glycol (PEG) and potassium dihydrogen phosphate (KH_2PO_4) to achieve phase separation. This is often considered the dominant advantage of ATPS because large-scale purification often requires large amount of chemicals.

Apart from low cost, polymers like PEG have the stabilizing effect on the biological activities and could maintain the structure of the target protein (Albertsson 1986). Due to its high water content, ATPS provides a biocompatible environment for proteins, enzymes and cell extracts (Agasoster 1998; Albertsson 1986; Gupta, *et al* 1999). ATPS is therefore viewed as an attractive alternative purification method due to its ability to combine several early processing steps (recovery, concentration and purification) into a single step process (Mazzola, *et al* 2008).

By using lower volume of ATPS to partition target product, the target material or product can be concentrated, and thereby increasing the yield. Moreover, recent advancement in ATPS technology has improved the recyclability of the phase components (Hustedt 1985; Veide, *et al* 1989). This could help to reduce pollution and other environmental impact of ATPS.

ATPS is also relatively more time-efficient compared to many purification methods. The time needed to form two-phase ranges from several minutes to several hours. Hence ATPS is able to produce more yield over time, apart from saving precious time when undergoing large-scale purification.

2.4 Purification of Carbon Nanotubes

The search for an effective purification method for SWCNT is one of the hottest research interests in the 21st century. An as-prepared SWCNT grown using the standard CVD process contains both semiconducting species and metallic species at a ratio of two to one. Each species of carbon nanotubes has its specific applications. Metallic species is commonly utilized in interconnect applications or making electronic sensors (Deng, *et al* 2007; Dresselhaus, *et al* 2005). Semiconducting species is usually integrated as the semiconducting channel of a field effect transistor (FET) (Jimenez, *et al* 2007; Ryu, *et al* 2010; Zhou, *et al* 2009). Therefore, the separation of S-SWCNT from M-SWCNT remains an important challenge in an effort to develop high-performance transistors. Many efforts have been made to separate the M-SWCNTs from the S-SWCNTs. Notable contributions include dielectrophoretic deposition (Krupke, *et al* 2006; Marquardt, *et al* 2006), DNA-assisted separation (Zheng, *et al* 2003), acid treatment (Yang, *et al* 2005), light-assisted oxidation (Yudasaka, *et al* 2003), amine interaction (Chattopadhyay, *et al* 2003), trapping of semiconducting SWCNTs using agarose gel (Tanaka, *et al* 2009) and microwave irradiation (Vazquez and Prato 2009).

In the work reported by Marquardt, short and dispersed SWCNTs were subjected to two different dielectrophoretic force fields. An electric field with field strength of $E_{rms}=3.5 \times 10^6$ V/m was then applied. They found out that mainly metallic species were attracted to the electrodes (Marquardt, *et al* 2006). They did not, however, quantify their findings in terms of purity and the yield of the purification.

The DNA-assisted separation is also an interesting methodology of separating M-SWCNT from S-SWCNT. SWCNT is found to be able to disperse in solution

containing single-stranded DNA. The modelling experiment showed that DNA could bind with SWCNT *via* π -stacking, which caused the DNA to wrap around the SWCNT (Zheng, *et al* 2003). In 2009, a new paper published by Xiaomin Tu *et al.* showed that DNA-assisted separation is also highly chiral-sensitive (Tu, *et al* 2009). A particular DNA sequence, poly(GT), formed ordered structures on SWCNTs. Therefore different DNA sequences could selectively wrap around SWCNT of different chirality, which could then be filtered out *via* ion chromatography (Tu, *et al* 2009). Nevertheless, the exorbitant price and the fragile nature of DNA render the DNA-assisted separation economically impractical for large scale purification. As of 1st April 2013, 0.1 milligram of DNA from human placenta costs RM 537.49 (Sigma Aldrich).

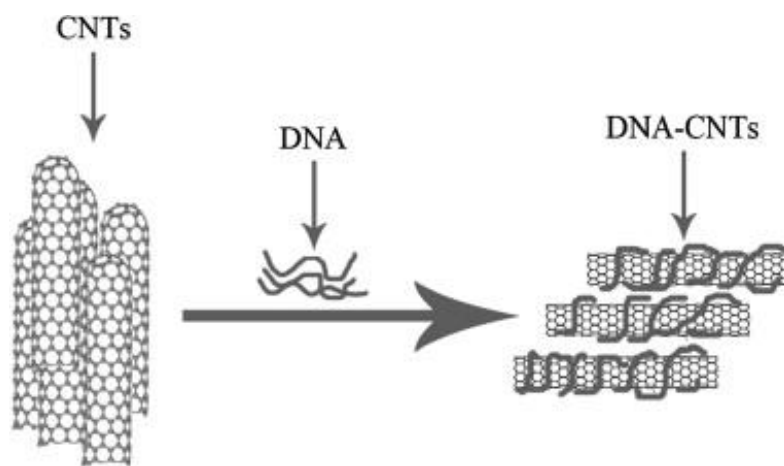


Figure 7 Schematic description of the formation of DNA-wrapped MWCNTs (Li, *et al* 2009)

The acid treatment method was developed by Cheol-Min Yang and his research group from the Ewha Womans University in 2005. The treatment involved dissolving SWCNT in a mixture of nitric acid and sulphuric acid at three volume ratios (1:9, 1:3, 1:2) for 12 and 48 hours, respectively. They reported that following the treatment, the metallic species with diameter less than 1.1 nm were removed while the semiconducting species remained intact. Since there were more available electron densities at Fermi level in M-SWCNT, therefore the positively charged nitronium ion (NO_2^+) would preferentially adsorb on the surface of M-SWCNT (Yang, *et al* 2005).

Nevertheless, the treatment of SWCNT using strong acid could result in unwanted carboxylic functionalities (Hamon, *et al* 2001).

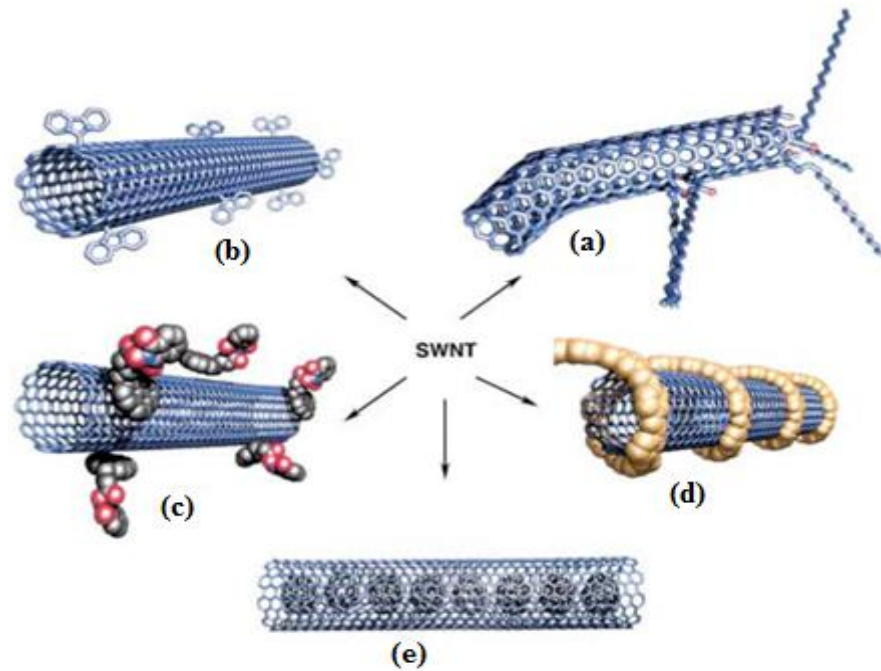


Figure 8 Functionalization possibilities for SWNTs: (a) defect-group functionalization, (b) covalent sidewall functionalization, (c) noncovalent exohedral functionalization with surfactants, (d) noncovalent exohedral functionalization with polymers, and (e) endohedral functionalization with, for example, C_{60} . For methods b-e, the tubes are drawn in idealized fashion, but defects are found in real situations (Hirsch 2002)

A highly cost effective purification of metallic SWCNTs is the use of combined diazonium and air-oxidation approach. A critical drawback of the method is the lengthy period required for the chemical reaction of SWCNTs with 4-bromobenzene diazonium to complete (Wu and Guan 2011).

A highly efficient and cost-effective purification method is the use of microwave radiation. In this method, the author exploited the intrinsic high dielectric constant of M-SWCNT (Kozinsky and Marzari 2006), which is due to its infinite polarizability (Benedict, *et al* 1995). On the contrary, the dielectric constant of S-SWCNT is relatively low, which ranges from 1 to 10 (Krupke, *et al* 2003). Due to its

high dielectric constant, M-SWCNT effectively absorbs much more microwave energy compared to S-SWCNT. This difference in absorbed energy can be applied to selectively destroy metallic species while retaining the semiconducting species. However, the thermal destruction of metallic SWCNTs using microwave induces random and uncontrollable damages to the neighbouring semiconducting SWCNTs (Shim, *et al* 2009). Therefore, a truly cost-efficient, scalable, time-saving and simple SWCNT separation protocol has yet to be developed.

2.5 Purification of Carbon Nanotubes using ATPS System

Industry demands fast, economic, high-yielding and efficient downstream processes for the partitioning and purification of SWCNTs. ATPS is an ideal technology to fulfil the above demands. This method can be easily scaled up and has been proven in wider biotechnological applications. The main motivation of this experiment is to develop a method in separating M-SWCNTs from S-SWCNTs by using an ATPS. To accomplish the objective, a new ATPS is developed using polyethylene glycol (PEG), dextran, *N*-methylpyrrolidone (NMP), cetyltrimethylammonium bromide (CTAB) and water. The concept of the research is simple: when an ATPS partitions into two distinct phases, certain species of carbon nanotubes will be attracted to one of the phases. It is critical that the S-SWCNTs are attracted to one of the components in an ATPS. The selective adsorption of amine onto S-SWCNTs is employed (Chattopadhyay, *et al* 2003; Kong and Dai 2001). NMP and CTAB are added to the system to disperse SWCNTs (Xiao, *et al* 2007; XIAO Qi 2007). The PEG/dextran system is chosen for this study because it is the most widely used ATPS system with rich reservoir of literature (Antov, *et al* 2004; Schindler and

Nothwang 2006). Moreover, dextran has also been reported to wrap around a SWCNT (O'Connell, *et al* 2001; Stobinski, *et al* 2008).

CHAPTER 3: EXPERIMENT DETAILS

3.1 Introduction

This chapter commences with the introduction of sources of material used in this experiment. Besides, step-by-step procedures for constructing the phase diagram are discussed as well. The optimization of the ATPS system using different molecular weight of polyethylene glycol (1,500~20,000 g/mol) is also highlighted in this chapter. The characterization techniques used in this experiment to study the structure, morphology and optical properties of separated nanotubes are also highlighted.

3.2 Experimental

3.2.1 Material

PEG (average molecular weight (M_w) of 1500 g/mol; 4000 g/mol; 6000 g/mol; 10000 g/mol; and 20000 g/mol), anhydrous NMP with 99.5% assay, cationic surfactant CTAB and dextran with average M_w of 40,000 g/mol were purchased from Sigma-Aldrich Co. (St. Louis, MO, USA). SWCNTs with tube diameter 0.7~0.9 nm were sourced from Southwest Nanotechnologies. Deionized water with 1% w/w CTAB was used throughout the experiment. All experiments were conducted within a class 10K clean room at temperature 19 °C.

3.2.2 Phase Diagram

Firstly, the phase-forming components for the research have to be chosen. Previously published information may serve as references for deciding the choices. Other choices could be used to replace existing phase components in the case of obtaining negative purification result. The process should be repeated until positive purification results are obtained (Benavides and Rito-Palomares 2008). Then, a phase diagram is constructed to produce a few ATPS for preliminary partitioning. Common ATPS parameters such as tie-line length (TLL) and volume ratio (V_R) are varied to produce the optimum purification (Rito-Palomares 2004; Rosa, *et al* 2010).

The predetermined quantities of PEG and dextran dissolved in deionized water were prepared in 15.0 mL vials. Then, 2.0 g of each polymer was added together to produce a final total weight of 4.0 g. The system was mixed thoroughly through gentle agitation. 0.5mg of pristine SWCNT was then added into the cloudy mixture. The system was then subjected to 10 minutes of centrifugation at 2000 rpm to induce phase separation. After the formation of two phases, the top and bottom phases were drawn out and the concentration of each species of SWCNT was evaluated using ultraviolet-visible spectroscopy. To gauge the effect of purification, the purification factors (P_F) of each species in both phases were evaluated.

The binodal curves for PEG 4000, 6000, 8000, 10000 and 20000-dextran system at pH 7.0 were obtained using turbidometric titration method as described by Hatti-Kaul (Hatti-Kaul 2000). Stock solutions of both polymers with known concentrations were prepared. The ATP systems were then prepared by mixing the two stock solutions together. Distilled water was added slowly into the turbid mixture followed by gentle agitation, until it turned into a transparent solution. At this point, the system reflects a homogenous phase. The weight of added distilled water was

determined to identify the curve's point. The process was repeated for different known weight composition systems to generate series points for binodal curve.

3.2.3 Separation Experiment

Several points were identified from the phase diagram for the separation experiment. A few vials containing different concentrations of PEG, dextran and NMP were prepared in several 7.0 ml vials. 0.5 mg of pristine carbon nanotubes is added into each of the vials and sonicated at 50W using the Thermo-6D Ultrasonic cleaner at 20 °C for 20 minutes. The SWNT powder would disperse in the solution following the ultrasonication. After thorough mixing by gentle agitation, the mixture was incubated at room temperature for 30 minutes to allow the phases to form.

3.2.4 Optimization and Post Treatment

In order to obtain the best yield, purification factor and dispersion of carbon nanotubes, the concentration of each phase forming components must be optimized. Several points were identified from the phase diagram and a few vials containing the plotted concentration of PEG, dextran and NMP were prepared. The volume ratios (V_R) of the top and bottom phases were measured and tabulated.

The two phases were drawn out using a pipette into two different vials. The concentrated solutions were then added with 2 ml of deionized water, followed by gentle agitation to reduce the viscosity of each phase. The solutions were then centrifuged at 40,000 rpm for 20 minutes. The supernatant was discarded, and 2 ml of deionized water with 1% CTAB was added to the precipitate to thoroughly disperse the SWNT. The cleaning process was repeated thrice to thoroughly get rid of contaminants

and excess polymers. The absorbance value of SWCNT for all the resultant volume ratios were recorded and tabulated. Then, the V_R that gives the highest absorbance value and purification factor was selected for characterization process.

3.3 Characterization of Carbon Nanotubes

The concentration of carbon nanotubes in the top and bottom phases was quantified by using absorption spectra obtained *via* Thermo Scientific Evolution 300 Ultraviolet-Visible-Near Infrared spectrophotometer with a scan rate of 120 nm/s. Micro-Raman spectroscopy was performed using a Renishaw inVia Raman microscope illuminated by a 514 nm wavelength laser. Atomic force microscopy images were obtained from the JPK Nanowizard 3 Atomic Force Microscope with a maximum scan range of 100 X 100 μm^2 . Besides, the content of the ATPS was analyzed using the Perkin Elmer Spectrum 400 Fourier Transform Infrared Spectrometer. The samples also underwent field-emission scanning electron microscopy *via* Hitachi SU 8000 FESEM. Lastly, X-ray photoelectron spectroscopy at the Synchrotron Light Research Institute (SLRI), Thailand with a 650 eV X-ray beamline was used for XPS characterization.

3.3.1 Ultraviolet-Visible Absorption Spectroscopy

The primary principle of the ultraviolet-visible (UV-Vis) absorption spectroscopy is the absorption of photons by matter. When a stream of photons passes through a matter, some photons are absorbed by the molecules of the matter, thus causing the resultant beam intensity to become lower than that of the initial beam.

Different materials have different absorbance band in different regions. Absorbance band for transition metals, for instance, lies in the range of visible light (400-700 nm). Organic compounds, on the other hand, have a variety of absorbance band depending on the nature of the bonds that form their molecules.

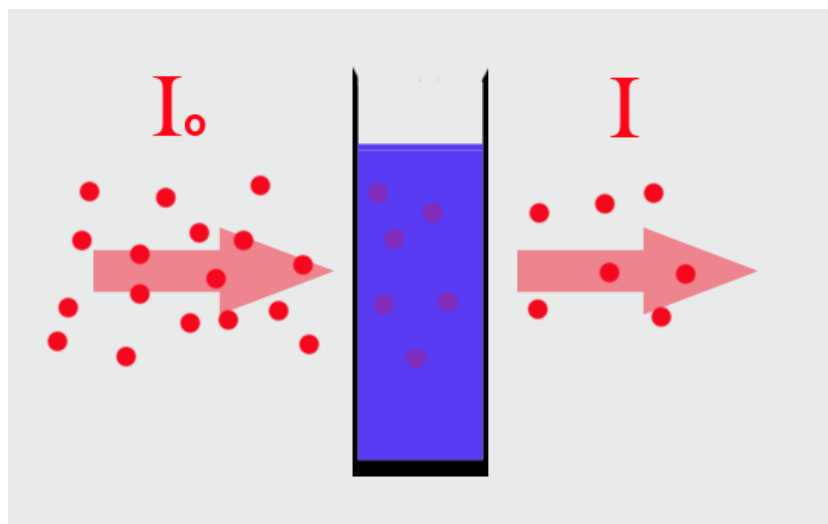


Figure 9 A monochromatic light, I_0 , passing through a cuvette. The light intensity decreases to I after passing through the cuvette due to adsorption

Optical transmittance, T is defined as the ratio of resultant light intensity, I , to the initial light intensity, I_0 :

$$T = \frac{I}{I_0} \quad (3)$$

The logarithm inverse of transmittance is defined as the optical absorbance A :

$$A = \log \left(\frac{I_0}{I} \right) = \log \left(\frac{1}{T} \right) \quad (4)$$

The law dictating the relationship between absorbance and concentration is the Beer-Lambert law. It states that absorbance is proportional to the concentration of the absorbing species, the path length (l , cm) and the concentration (c , mol/L) of the absorbing species:

$$A = \epsilon l c \quad (5)$$

In equation (5), ϵ represents the molar extinction coefficient ($\text{L mol}^{-1} \text{ cm}^{-1}$). It is the measure of the amount of light absorbed per unit concentration. The value of ϵ differs according to different absorbing species. Equation (5) shows that UV-Vis spectroscopy can be used to determine the concentration of the certain chemical in a solution, and thus identify different types of chemicals based on their distinctive curves.

In this work, the separated SWCNTs sample will be pipetted out and rinsed with deionized water. The sample will then be mixed with water with 1% CTAB to re-disperse the SWCNTs. The re-dispersed mixture will be dropped into a cuvette for the UV-Vis spectroscopy measurement.

UV-Vis spectroscopy is a widely utilized tool for the characterization of SWCNTs (Attal, *et al* 2006). The reduction in the size of the peak signifies the reduction of the M-SWCNT or S-SWCNT component in the sample (Fogden, *et al* 2012). Despite the large number of chemicals involved in the formation of ATP, they do not affect the resulting UV-Vis spectra. CTAB, for example, does not absorb light in the same wavelength region as that of SWCNTs (Attal, *et al* 2006). PEG has no UV chromophore, i.e. it is transparent and does not absorb light (Elliott, *et al* 2012). Dextran, too, does not possess characteristic absorbance in UV and visible region (Wang, *et al* 2010). Organic solvent NMP does have low UV chromophore. But its absorbance peaks at wavelength 229 nm, 304 nm and 321 nm (Opaprakasit, *et al* 2004), which is out of our minimum wavelength investigation which is 350 nm. Hence the peak intensity in the region between 350-750 nm, attributed to the optical transition between Van Hove Singularities, comes wholly from SWCNTs.

3.3.2 Micro-Raman Spectroscopy

Micro-Raman spectroscopy is a powerful tool for the characterization of SWCNT. The primary principle of Raman spectroscopy involves the interaction between light and matter, in which the light is inelastically scattered in a process known as the Raman Effect. The photons from a laser are focused at the sample, where they will interact with the molecules of the samples and are either reflected, absorbed or scattered.

Most of the elastically-scattered photons are of the same wavelength as the incident beam. A small number of the incident photons, however, are scattered with wavelength different to the incident beam. For the scattered photons, their wavelengths can either be shifted to higher or lower energy level, dubbed as blue or red shifted, respectively. The more common phenomenon is the red shift, which is also known as Stokes shift.

Apart from scattering, the photons interact with the electron cloud of the bonds present in the functional groups. This will then excite an electron into a virtual state. From there, the electron then relaxes into a less excited vibrational or rotational state. This relaxation of electron causes the release of photons, which is detected as Stokes Raman scattering. The energy lost is directly related to the functional group, the structure of the molecule, the types of atoms in that molecule and its environment. The information is then picked up and translated into Micro-Raman spectra.

In this work, the separated SWCNTs sample will be dropped on a piece of glass. The glass will then be put inside the sample chamber and illuminated by a green laser.

3.3.3 X-ray Photoelectron Spectroscopy

X-ray Photoelectron spectroscopy (XPS) was first used in the mid 1960s to probe the composition of elemental, chemical stoichiometry, chemical state, and electronic state of the elements of a material. It must be operated under ultra-high vacuum (UHV) to ensure smooth electron detection and to prevent sample contamination. The targeted material will be bombarded with an X-ray beam which will cause the electrons at the surface of the material to escape. Two quantities namely the kinetic energy and the number of electrons that escape are detected and analyzed. Since the bonding energy of electrons for each material is unique, hence it is possible to determine the type of material from which the electrons escape by determining the kinetic energy of the escaped electrons.

3.3.4 Fourier-Transform Infrared Spectroscopy

Fourier transform infrared spectroscopy (FTIR) is a technique for obtaining infrared spectra of absorption, emission, photoconductivity or Raman scattering of a solid, liquid or gas. The term *Fourier transform* means that a mathematical Fourier transform is required to transform the obtained information into spectrum.

The degree of absorption of the infrared beam at each wavelength is proportional to the number of absorbing molecules in the sample. This makes multicomponent quantitative analysis of mixtures possible. In order to perform multicomponent analysis, it is important to first obtain the reference spectra for all the individual components of a sample. A reference spectrum is a spectrum of a single component of known concentration. Chemical bonds such as C=O and C-C have their

very own signature spectra. Therefore it is possible to trace the presence and concentration of each individual component contained in a mixture.

Using the FTIR, it is possible to trace the different chemicals in a mixture. Therefore, it is an ideal instrument for determining the types of phase component in the top and bottom phase contained in this work.

3.3.5 Atomic Force Microscopy

Atomic Force Microscopy (AFM) is a type of high-resolution scanning probe microscopy. An AFM uses a cantilever—a sharp tip typically made of silicon or silicon nitride—to scan the surface of the sample. The radius of the tip of the cantilever is usually in the order of nanometers. When the tip approaches the surface of a sample, the forces acting on tip by the sample will cause the cantilever to deflect. The deflection will be measured *via* the reflection of a laser spot reflected from the top of the cantilever into a row of photodiodes.

3.3.6 Field Emission Scanning Electron Microscopy

The Field Emission Scanning Electron Microscopy (FESEM) is a useful surface morphological technique for the characterization of nanostructures. Unlike optical microscopes which can only view micron-size material, an electron microscopy gives an even higher resolution.

The electrons used for SEM are generated using two types of electron guns, namely the thermionic gun and field emission gun. The field emission (FE) gun is made up of a tungsten tip, usually less than 0.1 micron in diameter, which serves as the cathode and two anodes. It is much brighter than the thermionic electron gun because it

can produce up to three orders of magnitude greater electron density. When a potential difference is applied across the terminals, the electrons acquire enough energy to penetrate the energy barrier of tungsten tip into the vacuum. There are two anodes: extraction anode (0-5 kV) which extracts the electrons; and acceleration anode (1-50 kV) which accelerates the electrons. Electromagnetic lenses are used to focus the electron beam, while the scanning coil deflects the beam to the target by adjusting the current flowing past the radial-oriented coils. The electron beam interacts with the sample and signals are picked up by a detector which transforms the signals into digital images.

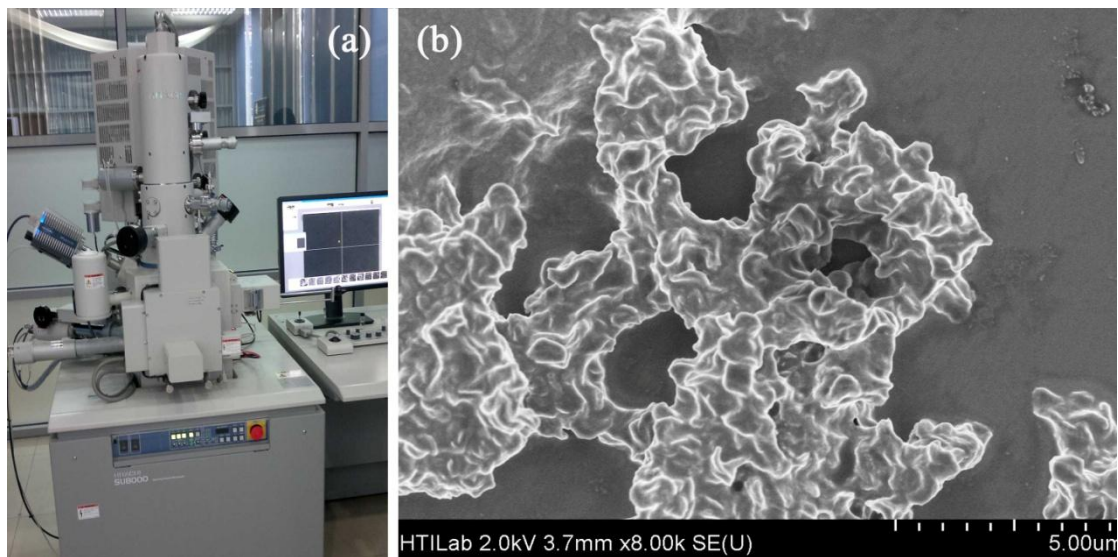


Figure 10 (a) Photograph of a Hitachi SU8000 FESEM; (b) FESEM image of a polymer

During an interaction, the incident electrons collide with the electrons of the sample to induce an inelastic scattering which ejects weakly-bonded electrons. The weakly-bonded electrons are also known as the secondary electrons, and the signals generated from these electrons are the ones used to generate FESEM images. This is because a single incident electron can generate more than 1000 secondary electrons. Nevertheless, the low energy of the incident electrons prevent them from penetrating

deeper into the sample, and thus the signals generated from secondary electrons are primarily those located close to the surface of the sample.

3.4 Calculations and Formulae

The volume ratio (V_R) was defined as the ratio of volume in the top phase (V_T) to the volume of the bottom phase (V_B) (10):

$$V_R = \frac{V_T}{V_B} \quad (10)$$

The purification factor (P_F) is described as the ratio of the metallic/semiconducting absorbance in the top phase to the pristine metallic/semiconducting absorbance (11):

$$P_F = \frac{\text{Metallic or Semiconducting top phase}}{\text{Metallic or Semiconducting}_{\text{pristine}}} \quad (11)$$

According to the Beer-Lambert's law shown in equation (5), absorption is proportional to the concentration of the absorbing species in a given material:

$$A = \epsilon lc \quad (5)$$

The total absorbance is the sum of each component absorbances:

$$A_{\text{total}} = A_1 + A_2 + A_3 + \dots A_n \quad (12)$$

Therefore, it is possible to sum up the absorbances for the metallic species and semiconducting species to obtain the total absorbance of the sample.

Using the definition of absorbance stated in equations (5) and (12), the partition coefficient, K , for different species of nanotubes is calculated according to Equation (13):

$$K = \frac{A_{Top}}{A_{Bottom}} \quad (13)$$

The specific activity (SA) of sample is described by Equation (14):

$$SA = \frac{M-SWCNT \text{ or } S-SWCNT \text{ absorbance}}{total \text{ absorbance}} \quad (14)$$

The purity of the resulting nanotubes is defined as the ratio of the absorbance of metallic species M_{11} to the absorbance of semiconducting species S_{22} :

$$Purity = \frac{Absorbance \text{ of } M_{11}}{Absorbance \text{ of } S_{22}} \quad (15)$$

The recovery yield of nanotubes (%) in each phase was computed according to equation (16):

$$Y_T(\%) = \frac{100}{1 + \left[\frac{1}{V_R * K} \right]} \quad (16)$$

where K is partition coefficient and V_R is the volume ratio.

CHAPTER 4: RESULTS AND DISCUSSION

4.1 Introduction

In chapter 4, the setup, construction and optimization of the aqueous two-phase system is discussed. The phase diagram of various PEG molecular weights is analyzed. The successfully separated two phases system is characterized using UV-Vis absorption spectroscopy, Micro-Raman spectroscopy, AFM, FESEM, XPS and FTIR spectroscopy. The UV-Vis absorption spectrum shows that there is a clear reduction of M-SWCNTs at the bottom phase. This is complemented by the Micro-Raman analysis which shows that there are less metallic species at the bottom phase. The Micro-Raman spectroscopy also shows that the D-band of the SWCNT spectrum is slightly more significant at the bottom phase. This means that the SWCNT has suffered some damage to the tube structure after the separation. AFM analysis shows that the SWCNTs are wrapped by polymer chains. The wrapping causes the SWCNTs to wriggle in worm-like shape. The FESEM result also provides substantial evidence of SWCNTs wrapped by polymers. The XPS analysis proves that the material presents around the SWCNT is polymer, because of the present of C—O peak in the XPS spectrum. Subsequent FTIR analysis shows that the top phase is dominated by the more hydrophobic polymer PEG, while the bottom phase is dominated by the hydrophilic polymer dextran. From the FTIR analysis it is found that NMP has an equal distribution in both phases, while the amine-bearing surfactant CTAB only appears at the bottom phase. A possible mechanism of the separation process is proposed at the end of this chapter.

4.2 Visual Analysis of SWCNT—ATPS

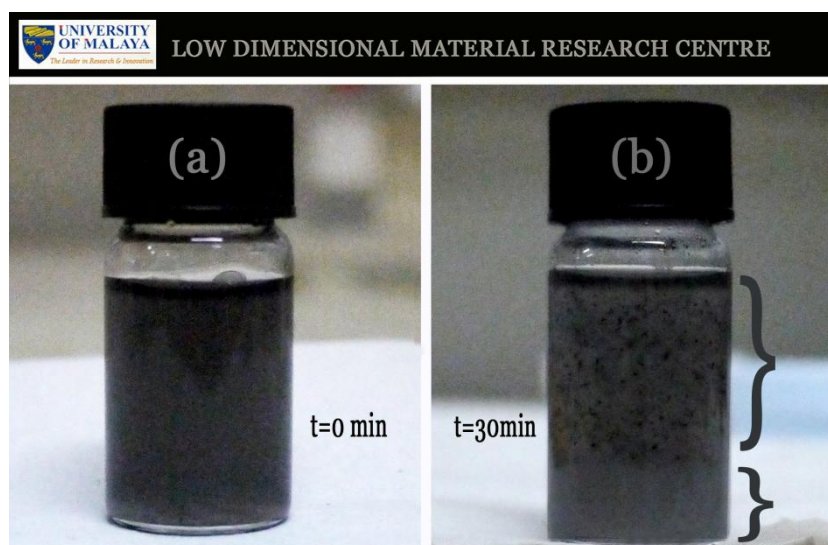


Figure 11 Photographs of ATPS made up of PEG-NMP/dextran-CTAB system before (a) incubation, and after (b) partitioning into two distinct phases

Immediately after sonication, the mixture of the solution was dark as shown in Figure 11(a). It should be noted that the pristine ATPS without SWCNTs is transparent. In approximately 30 minutes, two distinct phases were formed as shown in Figure 11(b). It is worth noting that prior to the formation of two phases the dispersion of SWCNTs in the mixture does not exhibit SWCNT bundles. The formation of SWCNT bundles occurred after the two-phase partition.

4.3 Phase Diagram

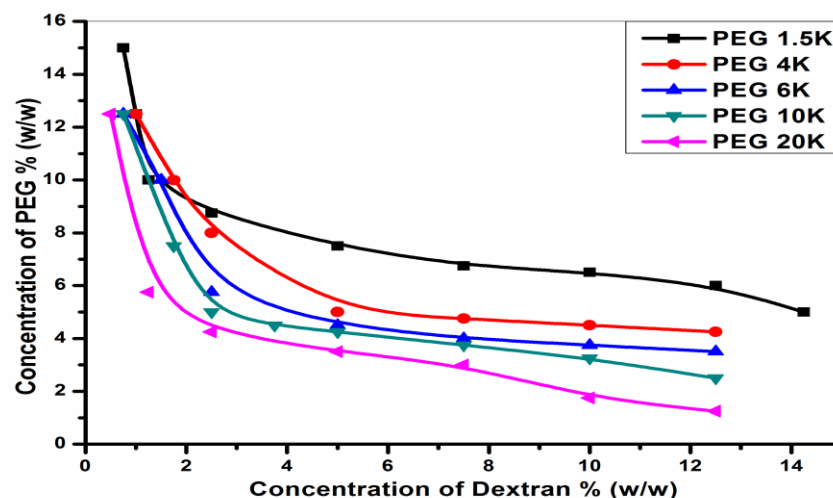


Figure 12 Phase diagram for PEG M_w 1500, 4000, 6000, 10000, and 20000 against dextran 40000

The binodal curves of various PEG (M_w 1500, 4000, 6000, 10000, 20000) against the single M_w dextran are shown in the phase diagram in Figure 12. It can be seen that all the binodal curves shift downwards to the dextran-axis as the M_w of PEG increases. This phenomenon is consistent with the work reported by Albertsson which claimed that the polymer with higher M_w requires less concentration to form two phases (Albertsson 1990a).

PEGs can dissolve easily in some organic solvents. In this experiment the PEGs were dissolved in NMP organic solvent as stock solutions. The PEG exhibited high solubility in NMP even when the M_w of PEG was increased. It is interesting to note that despite using NMP in place of water, the resultant binodal curves is in agreement with the prediction by Albertsson for PEG dissolved in water. The phase diagram shows that the quantity of polymer is needed to form two-phase reduces as the polymer M_w increases. This may result in the reduction of the operation cost while minimizing the impact on the environment.

4.4 Optimization Table

4.4.1 The effect of M_w on nanotubes partitioning

PEG	Concentration of PEG in NMP (% w/w)	Concentration of dextran in CTAB (% w/w)	K			Yield (%)		
			M_{11}	S_{22}	S_{33}	M_{11} top	S_{22} top	S_{33} top
4K	20.0	25.0	Salt-out	Salt-out	Salt-out	Salt-out	Salt-out	Salt-out
	15.0	25.0	Salt-out	Salt-out	Salt-out	Salt-out	Salt-out	Salt-out
	25.0	12.5	0.0546	0.0423	0.0510	32.9	27.6	31.5
	23.0	18.0	0.337	0.252	0.211	57.2	50.2	45.7
6K	25.0	15.0	0	0	0	0	0	0
	20.0	20.0	0.0707	0.0590	0.0497	17.5	15.0	12.9
	17.5	21.0	0.696	0.671	0.460	61.9	60.9	51.7
	23.0	18.0	0.187	0.212	0.184	51.5	54.6	51.0
10K	20.0	15.0	0.221	0.205	0.234	47.0	45.1	48.4
	18.0	20.0	0.117	0.138	0.119	21.4	24.4	21.7
	15.0	15.0	0.280	0.277	0.271	52.8	52.6	52.0
	22.0	15.0	0	0	0	0	0	0
20K	13.0	15.0	0.201	0.150	0.256	31.9	25.9	37.4
	17.5	20.0	0.0656	0.0473	0.0512	10.9	8.07	8.68
	15.0	15.0	0.0349	0.0291	0.0331	9.47	8.02	9.03
	18.0	12.5	0.108	0.0820	0.107	38.0	31.7	37.7

Table 1 The effect of M_w on SWCNT partitioning

Table 1 indicates that the partitioning of SWCNTs in PEG-NMP/dextran-CTAB system is dependent on the M_w of PEG. From the table, we can observe that the two highest partition coefficient, K (0.6957), and yield (61.85 %) value are obtained from the experiments involving the 6000 and 10000 M_w PEG, respectively. The M_w 10000 PEG shows a more promising and consistent results compared to M_w 4000 and 20000 PEGs, but its yield (46.96) and K (0.2343) values are lower than that of M_w 6000 PEG. The other two polymers, i.e. M_w 4000 and 20000 PEGs give low yield and K values. The M_w 4000 PEG exhibited two salt-out events at PEG 20% (w/w)/dextran 25% (w/w) and PEG 15% (w/w)/dextran 25% (w/w). But salt-out did not occur for high PEG/dextran concentration in the M_w 6000 PEG experiment, for example the PEG 20% (w/w)/dextran 20% (w/w). This shows that as PEG M_w increases, the systems become more resilient against salt-out. It is evident that nanotubes-partitioning using certain M_w

of PEG could lead to high K and yield values. Therefore, the PEG that gives the highest yield and K value, PEG 6000/dextran system, was chosen for further study.

4.4.2 The effect of V_R on nanotube partitioning coefficient, purity, specific activity and purification factor

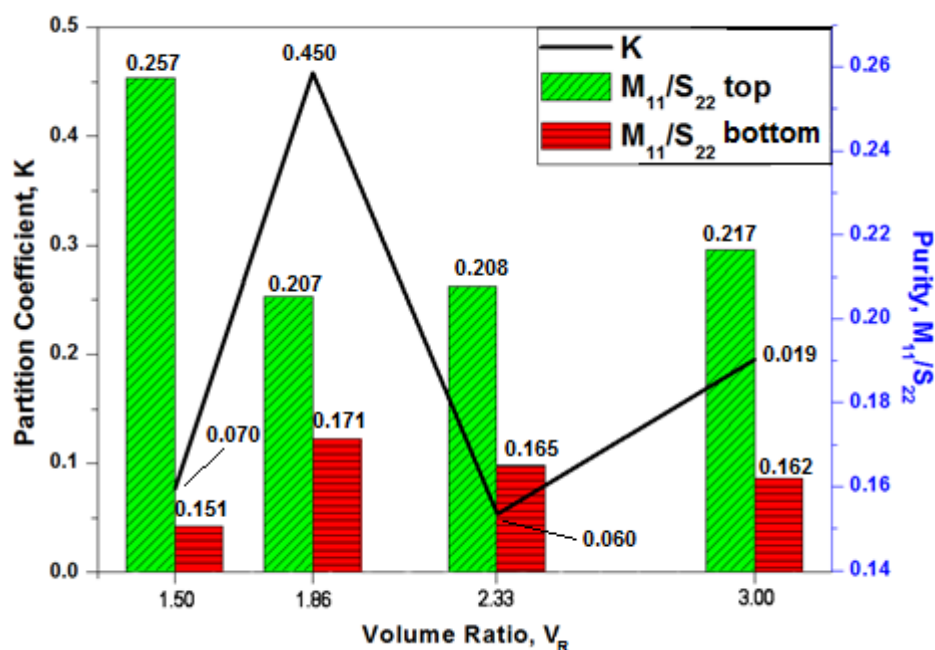


Figure 13 The effect of V_R on the partition coefficient K and the purity (M_{11}/S_{22}) of SWCNTs

The K and purity of SWCNT gauged at different V_R is shown in Figure 13. The ATPS was constructed by mixing PEG with concentration ranging from 12-15% (w/w) and dextran concentration 18-25% (w/w). Note that the K value for M-SWCNT reaches its highest value (0.4581) at V_R 1.86. The value then drops to 0.0536 before rising again to 0.1956 at V_R 3.0. Meanwhile, we can observe from the column that there is a huge difference in terms of purity for V_R 1.5. The ratio of M_{11}/S_{22} in the top phase for V_R 1.5 reaches 0.2574 compared to 0.1507 in the bottom phase. This means that there are more metallic species residing in the top phase compared to the bottom phase.

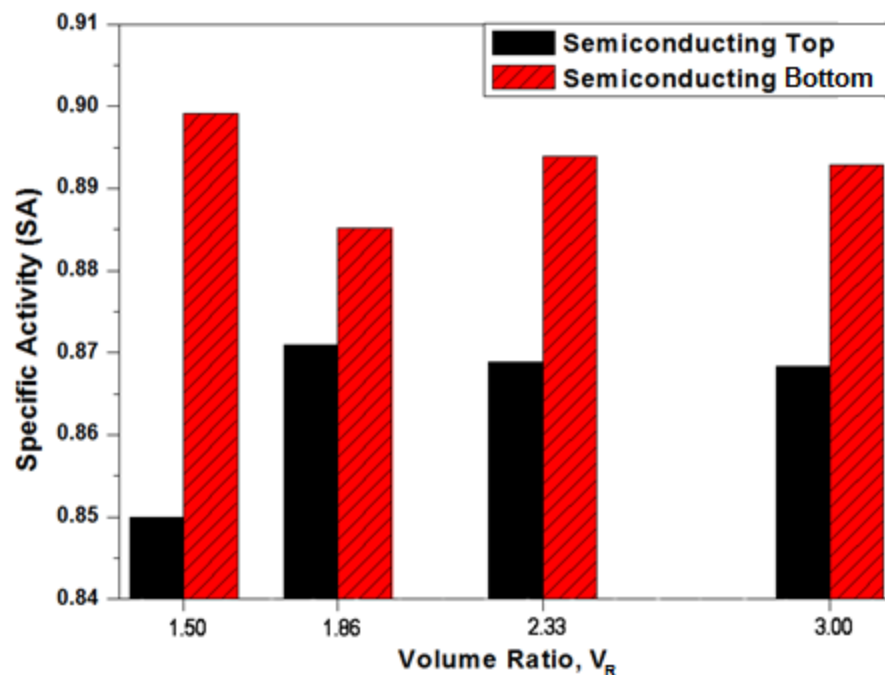


Figure 14 The effect of V_R on the specific activity of S-SWCNT in top and bottom phases

Figure 14 shows the effect of different V_R on the specific activity of semiconducting SWCNT in both phases after purification. We can see that there is a clear difference between the top and bottom phases especially for $V_R=1.5$. Theoretically, lipase partitioning behavior will not be affected by changes of V_R because the relative partitioning of individual enzyme will stay the same (Ashipala and He 2008). Therefore it is interesting to see if it also holds for SWCNT. The results indicate that K shows a random pattern with the increment of V_R (Figure 13). This means that the partitioning behavior of SWCNT does not depend on the change of V_R .

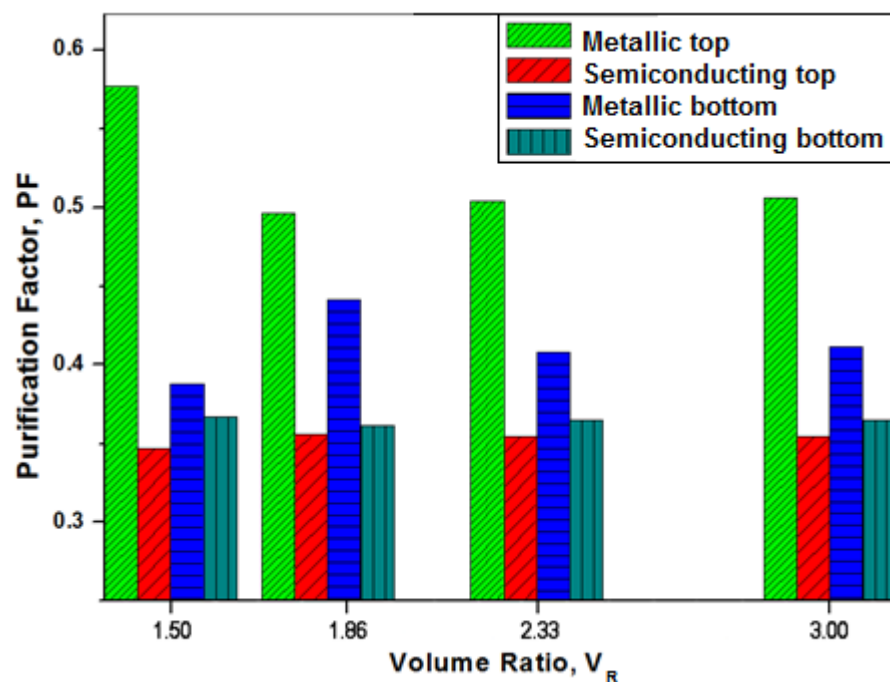


Figure 15 The effect of V_R on the purification factor of all the species of SWCNT in both phases

From Figure 15, we can see that the species that exhibited the largest difference between the top and bottom phase is the metallic species at $V_R=1.5$. The semiconducting species, however, shows relatively less drastic changes. This means that there is not much change in term of semiconducting concentration in the two phases for the said V_R . This contradicts with the reports reported by various authors that amine attracts semiconducting species (Chattopadhyay, *et al* 2003; Kong and Dai 2001) instead of metallic species. The reason for this could be that amine actually adsorb more strongly on metallic species compared to semiconducting species, as reported by Maeda in 2005 (Maeda, *et al* 2005) who suggested that the complex of amine and as-prepared M-SWCNTs may have higher solubility in organic solvents compared to S-SWCNTs.

4.4.3 The effect of the concentration of NMP and water on V_R , K, yield, SA, PF, and purity

The inclusion of NMP in the system serves two functions: it is an effective dispersing agent of SWCNTs; it is an amide. Amine has been reported to attract S-SWCNT (Chattopadhyay, *et al* 2003). Apart from NMP organic solvent, the CTAB amine-bearing surfactant was also included in our experiment. 1% (w/w) CTAB is added to deionized water to facilitate the dispersion of SWCNT. Therefore it is important to gauge the effect of the concentration of NMP and water on the separation of M-SWCNT from S-SWCNT.

PEG 6K (15% w/w)	Dextran 40k (20% w/w)	V_R	K			Yield (%)		
			M_{11}	S_{22}	S_{33}	M_{11}	S_{22}	S_{33}
4.50g	2.00g	Salt-out	Salt-out	Salt-out	Salt-out	Salt-out	Salt-out	Salt-out
4.00g	2.00g	Salt-out	Salt-out	Salt-out	Salt-out	Salt-out	Salt-out	Salt-out
3.50g	2.00g	Salt-out	Salt-out	Salt-out	Salt-out	Salt-out	Salt-out	Salt-out
3.00g	2.00g	3.00	0.0344	0.0328	0.0319	9.35	8.96	8.74
2.50g	2.00g	3.00	0.0517	0.0586	0.0622	13.4	14.9	15.7
2.00g	4.50g	1.00	0.0595	0.0487	0.0512	5.62	4.65	4.87
2.00g	4.00g	1.00	None	None	None	None	None	None
2.00g	3.50g	1.08	None	None	None	None	None	None
2.00g	3.00g	1.25	0.0851	0.0830	0.0770	9.61	9.40	8.78
2.00g	2.50g	1.86	0.0598	0.0515	0.0533	9.99	8.74	9.00
4.50g	2.50g	4.00	0.0735	0.0673	0.0690	22.7	21.2	21.6
4.00g	2.50g	5.67	0.325	0.318	0.356	64.8	64.3	66.9
3.50g	2.50g	3.00	0.0509	0.0453	0.0609	13.2	12.0	15.5
3.00g	2.50g	3.00	0.208	0.219	0.198	38.4	39.7	37.3
2.50g	4.50g	1.22	None	None	None	None	None	None
2.50g	4.00g	1.50	None	None	None	None	None	None
2.50g	3.50g	1.86	None	None	None	None	None	None
2.50g	3.00g	2.33	0.0676	0.0648	0.0496	13.6	13.1	10.4
4.50g	3.00g	3.00	0.195	0.184	0.266	36.9	35.5	44.4
4.00g	3.00g	3.00	0.514	0.468	0.475	60.7	58.4	58.7
3.50g	3.00g	2.33	0.215	0.191	0.190	33.4	30.8	30.7
3.00g	4.50g	1.50	0.174	0.215	0.126	20.7	24.4	15.9
3.00g	4.00g	1.86	0.289	0.283	0.285	34.9	34.4	34.6
3.00g	3.50g	2.13	0.140	0.136	0.153	23.0	22.4	25.4

Table 2 The effect of the concentration of NMP and water on V_R , K and yield

PEG 6K (15% w/w)	Dextran 40K (20% w/w)	Specific activity				Purification index				M_{11}/S_{22}	
		M-SWCNT top	S-SWCNT top	M-SWCNT bottom	S-SWCNT bottom	M-SWCNT top	S-SWCNT top	M-SWCNT bottom	S-SWCNT bottom	top	bottom
4.50g	2.00g	None	None	None	None	None	None	None	None	None	None
4.00g	2.00g	None	None	None	None	None	None	None	None	None	None
3.50g	2.00g	None	None	None	None	None	None	None	None	None	None
3.00g	2.00g	0.109	0.364	0.104	0.896	0.420	0.149	0.400	0.366	0.172	0.164
2.50g	2.00g	0.0922	0.353	0.105	0.895	0.354	0.144	0.403	0.366	0.142	0.161
2.00g	4.50g	0.121	0.348	0.103	0.897	0.466	0.142	0.395	0.366	0.186	0.152
2.00g	4.00g	None	None	None	None	None	None	None	None	None	None
2.00g	3.50g	None	None	None	None	None	None	None	None	None	None
2.00g	3.00g	0.102	0.328	0.0977	0.902	0.391	0.134	0.376	0.368	0.151	0.148
2.00g	2.50g	0.113	0.337	0.100	0.900	0.436	0.138	0.384	0.368	0.171	0.148
4.50g	2.50g	0.110	0.346	0.102	0.898	0.421	0.141	0.392	0.367	0.168	0.153
4.00g	2.50g	0.102	0.358	0.103	0.897	0.393	0.146	0.396	0.366	0.159	0.156
3.50g	2.50g	0.109	0.391	0.106	0.894	0.419	0.160	0.408	0.365	0.179	0.159
3.00g	2.50g	0.0977	0.320	0.100	0.900	0.376	0.130	0.385	0.367	0.144	0.151
2.50g	4.50g	None	None	None	None	None	None	None	None	None	None
2.50g	4.00g	None	None	None	None	None	None	None	None	None	None
2.50g	3.50g	None	None	None	None	None	None	None	None	None	None
2.50g	3.00g	0.103	0.308	0.0933	0.907	0.396	0.126	0.359	0.370	0.149	0.143
4.50g	3.00g	0.0986	0.381	0.102	0.898	0.379	0.155	0.394	0.367	0.159	0.150
4.00g	3.00g	0.0956	0.310	0.0882	0.912	0.368	0.127	0.339	0.372	0.139	0.126
3.50g	3.00g	0.107	0.307	0.0964	0.904	0.412	0.125	0.371	0.369	0.155	0.138
3.00g	4.50g	0.0837	0.316	0.0877	0.912	0.322	0.129	0.337	0.372	0.122	0.152
3.00g	4.00g	0.0978	0.318	0.0962	0.904	0.376	0.130	0.370	0.369	0.144	0.141
3.00g	3.50g	0.102	0.356	0.102	0.898	0.391	0.145	0.392	0.367	0.158	0.153

Table 3 The effect of the concentration of NMP and water on the SA, PF and purity

From Tables 2 and 3, we can see that generally, the purity of the resultant nanotubes is independent of the V_R . The mixing of PEG stock solution 15% (w/w) with dextran stock solution 20% (w/w) at various weighs will increase the amount of NMP and water significantly. From the results, 4.0 g of PEG 15% (w/w) mixed with 2.5 g of dextran 20% (w/w) gives the highest yield (64.79%), but the purity for the top phase is identical to that of the bottom phase. This means that despite the high yield value, there is no separation of the two species of nanotubes. As for partition coefficient, K, the highest K value (0.5139) comes from the mixture of 4.0 g PEG 15% (w/w) with 3.0 g dextran 20% (w/w). However, the difference in purity for the top and bottom phase for this system is also insignificant. Other results such as PF and SA also do not change much. This shows that the change in NMP concentration will not affect the overall outcome of the separation, but the changes in the concentration of PEG and dextran will.

4.5 Ultraviolet-Visible Absorption Spectroscopy

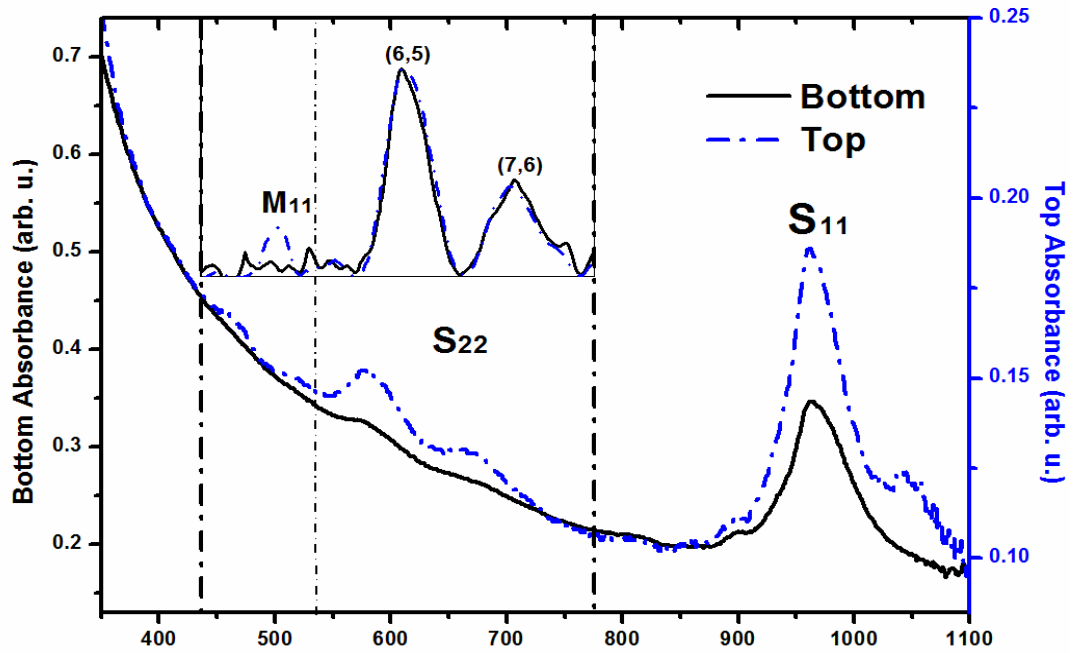


Figure 16 UV-Vis spectra for both top and bottom phase

UV-Vis absorption spectroscopy measurement for the top and bottom phases is shown in the above figure. The wavelength of investigation ranges of 350 nm to 1100 nm, but the focus of the work is in the region between 350 nm and 750 nm. The inset of Figure 16, which will be discussed in detail as Figure 17, shows the baseline-subtracted spectra of the top and bottom phase from 430 -780 nm. The peak at the 450 nm signifies the metallic species, denoted as M_{11} , while the semiconducting species exhibits two peaks, i.e. 550-650 nm and 950-1050 nm, denoted as S_{22} and S_{11} , respectively. The area under each peak is related to the concentration of the corresponding species, as given by Beer-Lambert law in equation (5). The ratio of M_{11}/S_{22} therefore presents a good measure of the relative decrement or increment of the two species in the sample.

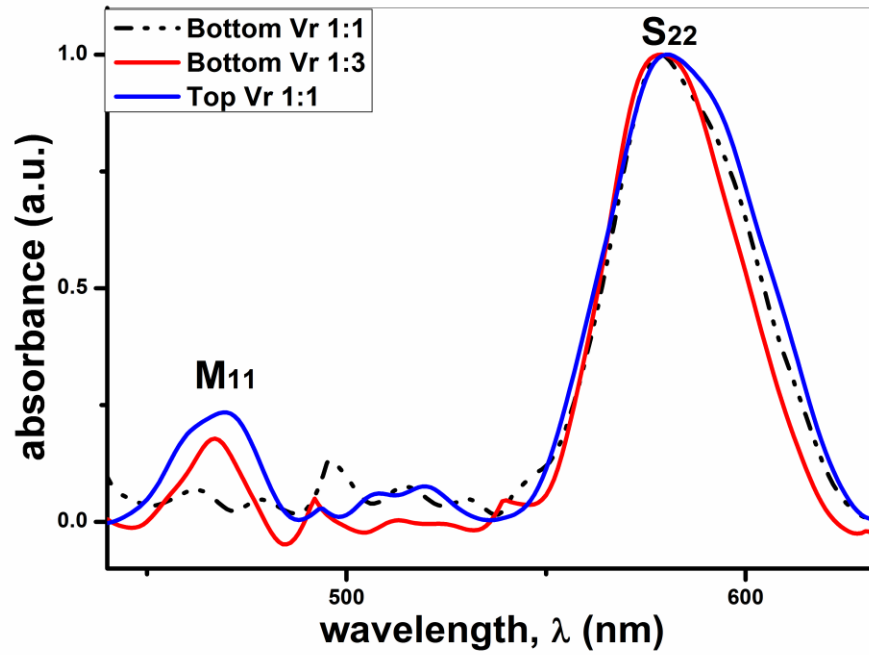


Figure 17 Baseline-subtracted spectra of the top and bottom phases from 430 nm-650 nm

To ease the discussion on the changes of M-SWCNT and S-SWCNTs, the 450 nm-650 nm region where M_{11} and S_{22} are located will be magnified and focused at. The resultant curve is baseline-subtracted to magnify the peaks of metallic and semiconducting SWCNTs. Figure 17 shows the baseline-subtracted-peaks in the 430 nm-650 nm region normalized at S_{22} peak at 581 nm. It can be clearly seen that for $V_R=1:1$, there is an enrichment of M_{11} peak, i.e. there are more M-SWNT in the top phase, whereas both the semiconducting peaks S_{11} for top and bottom phases remain roughly the same. For the bottom phase of $V_R=1:1$, despite the high absorbance shown by S_{22} peak, the signal from the M_{11} peak is undetected, but the M_{11} for bottom phase $V_R=1:3$ is comparable to the M_{11} for bottom phase $V_R=1:1$. The fluctuation seen in region 400-500 nm is the result of the small background noise after baseline-subtraction.

4.6 Micro-Raman Spectroscopy

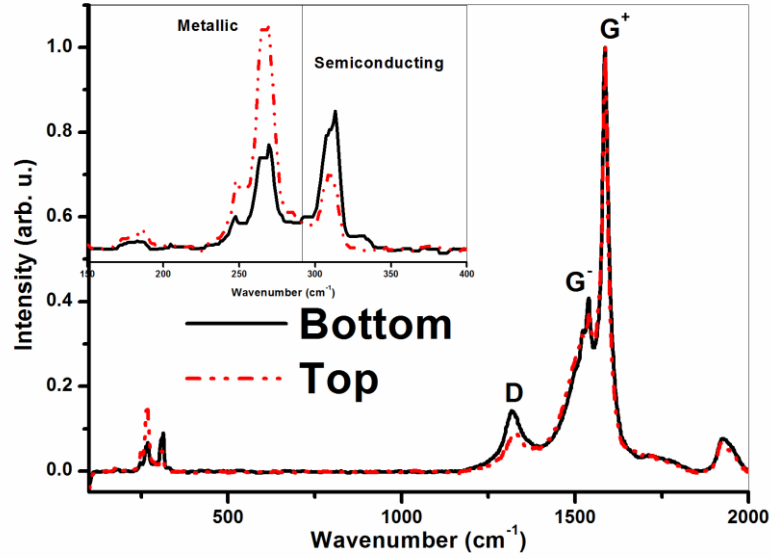


Figure 18 Raman spectra for top and bottom phases normalized at G^+ peak (1581 cm^{-1}). The inset shows the RBM region of the Raman spectra. The RBM metallic peaks for the top phase are more intense compared to the bottom phase

Micro-Raman spectroscopy is a powerful tool for the characterization of SWCNTs, from which their diameter and electronic properties can be estimated (Dresselhaus, *et al* 2002). Raman spectra of the samples were measured with laser wavelengths of 514.5 nm. From the analysis of radial breathing modes (RBM), the diameters of the SWCNTs are estimated to be 0.7-0.9 nm. A detailed study of the plots by Kataura *et al.* allows us to assign and identify the chirality and species for each peak (Kataura, *et al* 1999). The frequency of the RBM is the monotonic function of the diameter. The position of the peaks and the diameter of different chirality of SWCNTs can be calculated *via* equation (17)

$$\omega_{RBM} = \frac{c_1}{d_t} + C_2 = \frac{\pi C_1}{a_c - c\sqrt{3(n^2 + nm + m^2)}} + C_2 \quad (17)$$

where ω_{RBM} is the mode frequency, $a_{\text{c-c}} = 0.144\text{nm}$, d_t is the diameter of the tube in nanometer, n and m are integers of the vector equation and the while C_1 and C_2 are empirically derived parameters. Previous work by Strano et al. yielded C_1 as 223.5 and C_2 as 12.5 cm^{-1} (Strano, *et al* 2003). Calculation based on equation (17) and comparison with Kataura plot yielded RBM wavenumbers between $180\text{-}300\text{ cm}^{-1}$ as peaks of M-SWCNTs species, whereas the S-SWCNTs have RBM wavenumbers in the range between $300\text{-}400\text{ cm}^{-1}$. Calculation by Jorio et al. shows that the dominant metallic species in this pristine carbon nanotube is the (7,4) species, followed by (8,5), (10,1) and (9,3) (Jorio, *et al* 2005).

Figure 18 shows the corresponding Raman spectra for the top and bottom phase SWCNT normalized at 1581 cm^{-1} . It can be seen from the RBM that the metallic peaks for the top phase are more intense compared to the bottom phase (inset of Figure 18). In contrast, the semiconducting peak for the bottom phase is more intense than that of top phase.

The region around $1500\text{-}1600\text{ cm}^{-1}$ is called the G-band. It is related to the lattice C—C stretching vibrations (Kukovecz, *et al* 2002). This property can also be used to gauge the level of purity of SWCNT. The broadening of G⁺ band indicates the presence of metallic species (Haroz, *et al* 2011). It is evident from Figure 18 that there is a slight broadening of G⁺ band for the top phase sample. The region around 1280 cm^{-1} to 1300 cm^{-1} represents the D-band. The intensity ratio of G band to D band offers a quick way to evaluate the purity and defect density of the carbon nanotubes (Miyata, *et al* 2011). The spectra shown in Figure 18 show that the signal of D band for the bottom phase is slightly stronger than that of the top phase. Hence a higher intensity D band in the bottom phase signifies a slightly higher degree of defect imparted on the tubes in the top phase. Hence, both micro-Raman and UV-Vis-NIR results indicate that the

metallic species are indeed more dominant in the top phase compared to the bottom phase.

4.7 X-ray Photoelectron Spectroscopy Analysis

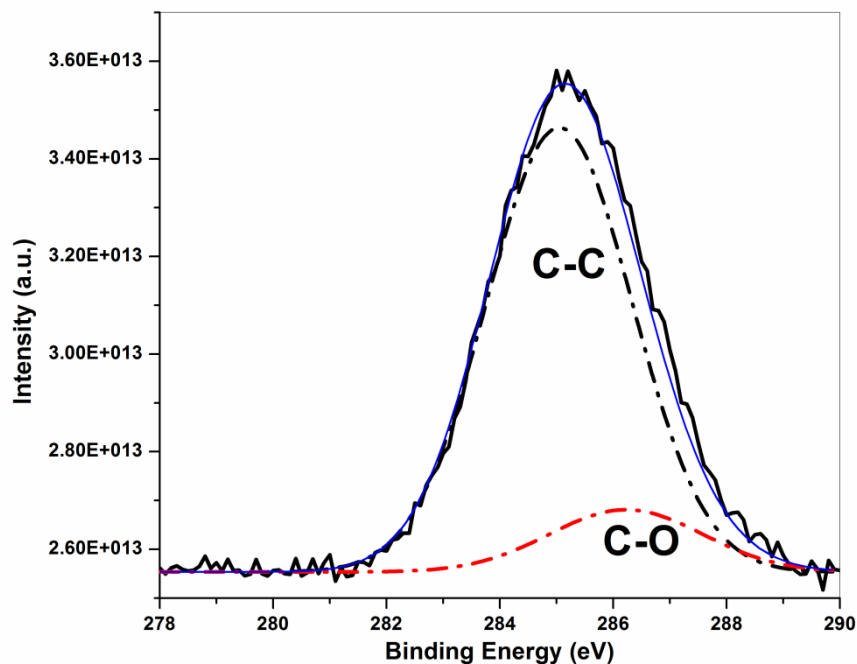


Figure 19 XPS of SWCNT and polymer

XPS analysis has been done to probe and investigate the presence of polymer in and around the SWCNT sample. The XPS analysis was done at SLRI, Thailand, with a 650 eV X-ray beamline. Fitting of the asymmetrical graph shows that there are two peaks. From the data shown in Figure 19, it is clear that the two peaks shown are at 285.0 eV and 286.2 eV; the former is attributed to the C—C bond while the latter comes from C=O bond.

Since carbon nanotubes are made entirely of carbon atoms, the C—C bond can be attributed to the carbon atoms from the carbon nanotubes. This is supported by an earlier results reported by Lee et al. which show that a typical XPS spectrum of the carbon 1S centres at 285.0 eV (Lee, *et al* 2001). Meanwhile, the peak centred at 286.2

eV is assigned to the C—O bond (Akhavan, *et al* 2009; Chen, *et al* 2009). The result is very close to the 286.4 eV published by the same group (Lee, *et al* 2001) mentioned above. Therefore it is clear that there is one oxygenated component present around the C—C component. The C—O bond is a contribution from polymer, which in this case could be either PEG or dextran because there is no oxygen atom in carbon nanotube, and hence it is not possible for C—O to originate from carbon nanotubes. This indicates that the polymer is enveloping the SWCNTs.

4.8 Fourier-Transform Infrared Spectroscopy

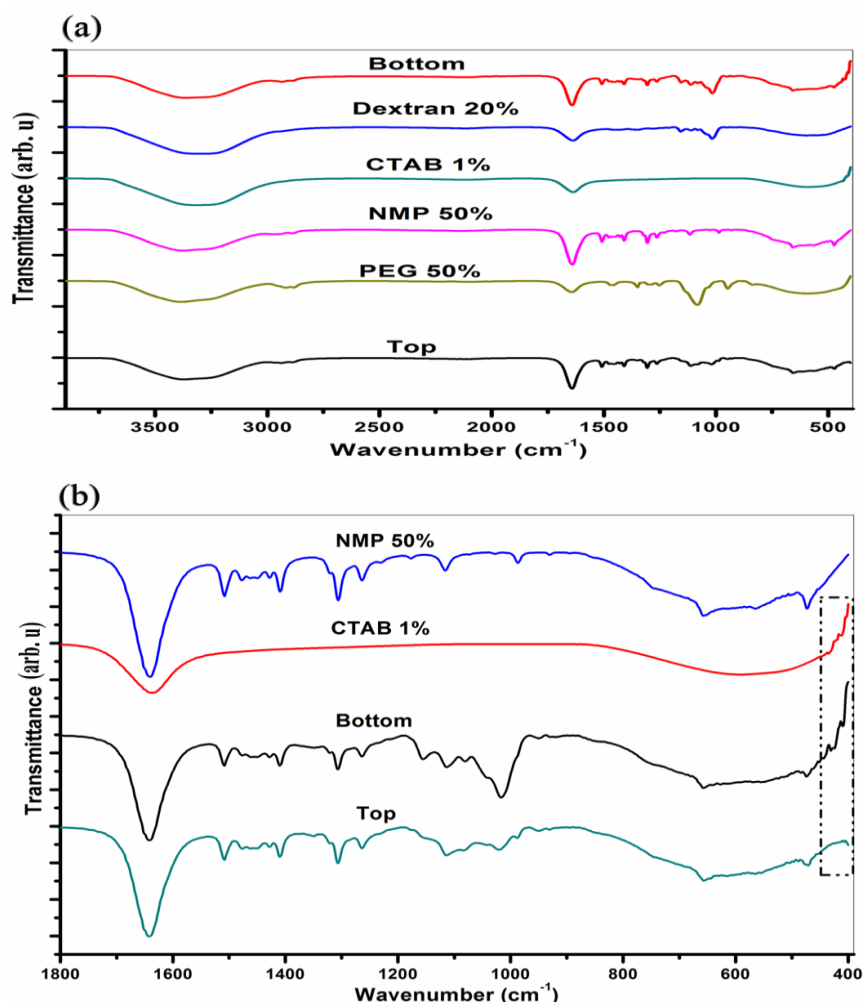


Figure 20 (a) FTIR spectra of all the constituents of the ATPS from 1800 cm^{-1} to 400 cm^{-1} (b) of NMP 50% w/w, CTAB 1% w/w, bottom phase and top phase. There is a clear indication of CTAB in the bottom phase as shown in the dashed rectangle

By using FTIR spectroscopy, the contents of the two phases were investigated. From the FTIR results shown in Figure 20 (a), it can be seen that the bottom phase contains a strong signal from dextran at 1000 cm^{-1} . Since PEG is more hydrophobic than dextran (Albertsson 1986), water tends to aggregate in the bottom phase. The FTIR curves in Figure 20 (b) show that signals from NMP organic solvent are present in both phases, which mean that the selective enrichment could not be due to NMP. CTAB, an amine-bearing surfactant, is present in the bottom phase but not detected in the top phase. The signal of CTAB can be seen in the bottom phase and compared clearly in Figure 20 (b) in the rectangular dotted box. Since the spectra obtained from the UV-Vis and Micro-Raman analyses show that the S-SWCNT is present in the bottom phase, hence it is possible that the selectivity of S-SWCNTs is attributed to CTAB.

4.9 Atomic Force Microscopy

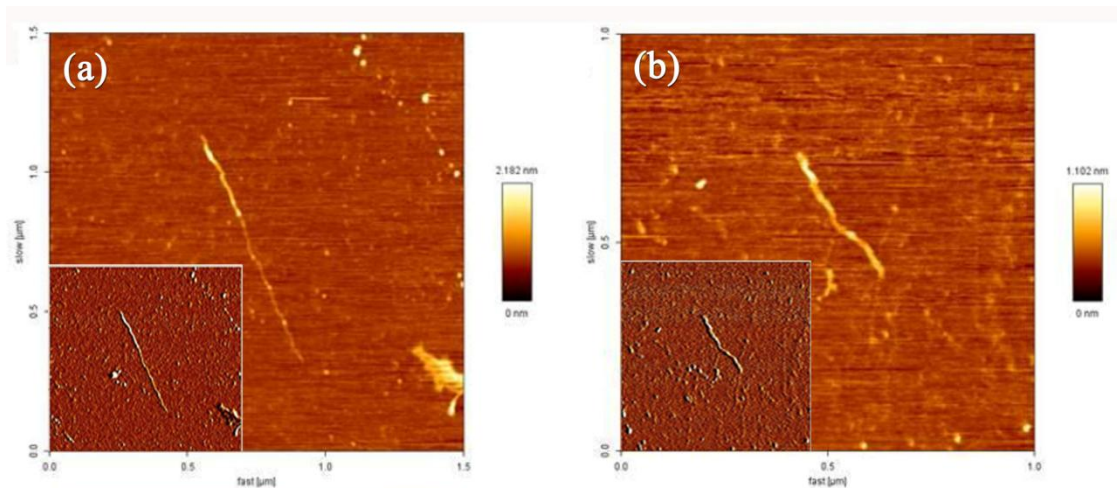


Figure 21 AFM height images of SWCNT extracted from the bottom phase. Figures (a) and (b) are two different spots on a same sample. The inset of both images shows the corresponding amplitude images

The AFM images of two single strand of SWCNT extracted from the bottom phase of the ATPS are shown in Figure 21. Both figures show the height images whereas the insets show the corresponding amplitude images. From the images, we can see a strand of SWCNT with bright contrast. AFM does not provide information on the species of the SWCNT, but the UV-Vis and Micro-Raman analyses show that S-SWCNT is more dominant in the bottom phase. Cross-section analysis indicated the height of the SWCNT in Figure 21 is approximately 0.7 nm, which is in agreement with the figure presented by the manufacturer of the SWCNT, Southwest Nanotechnologies.

It is interesting to note that the two strands of SWCNT shown in Figures 30 (a) and (b) are not slick, long and sturdy ropes. Instead, both exhibit worm-like wriggling as if they are wrapped by a polymer chain. In fact there is an earlier publication which shows that SWCNT wrapped by polymer will exhibit such wriggling phenomenon (Kumar, *et al* 2012). This corresponds well with the fact that dextran used in the ATPS can act as long polysaccharide chains that wrap around a SWCNT (Stobinski, *et al* 2008). The non-covalent wrapping of a SWCNT is favourable because it preserves the physical properties of the SWCNT (Kumar, *et al* 2012).

4.10 Field Emission Scanning Electron Microscopy

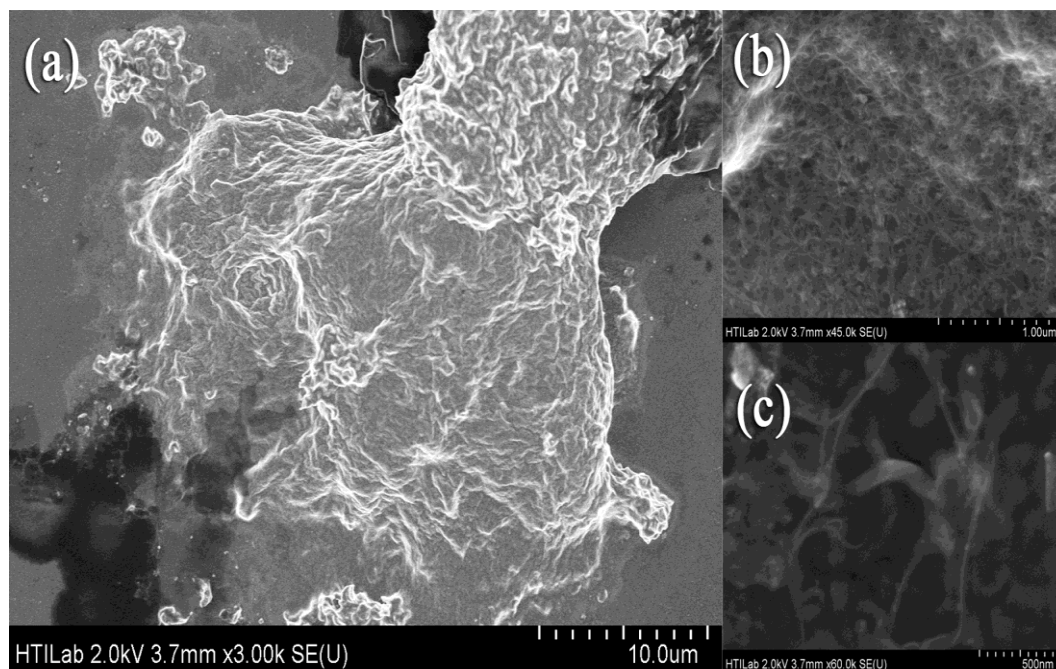


Figure 22 FESEM images of (a) PEG, (b) close-up look at the PEG, where strands of SWCNTs can be found, and (c) single strand of SWCNT

FESEM images of the samples are shown in Figure 22. The huge clump of material observed in image (a) is the dried-up polymer which is either dextran or PEG. The reason for this uncertainty is that for an ATPS, all chemicals will be present in both phases. Although it is evident from literature and experiment that dextran is more dominant in the bottom phase, but there are still traces of PEG present in the bottom phase.

It can be clearly seen from Figure 22 (b) that the SWCNTs are distributed quite evenly in the polymer. The area surrounding the polymer was found to contain no traces of carbon nanotubes. The area surrounding the polymer was found to contain no traces of carbon nanotubes. When looked closer, the tubes appeared to have some nanoparticles attached to its sidewall, as can be seen from Figure 22 (c). Those

nanoparticles could be the micelles of surfactant CTAB. Surfactant molecules form micelles when the concentration of the surfactant goes beyond the critical micellar concentration (CMC) (Gaidamauskas, *et al* 2010). When this happens, the hydrophobic tails of several surfactant molecules will bond together forming a ball of molecules called micelle. In this formation, the hydrophilic head of surfactant molecules will be pointing out towards the water-rich environment, shielding the hydrophobic tail within the micelle, as shown in Figure 23. With the presence of these CTAB nanoparticles on the SWCNT, it could possibly explain the reduced dispersion of SWCNT in the upper phase as shown in Figure 20(b). When the molecules of CTAB form micelle instead of attaching their hydrophobic tails into SWCNT sidewall, the number of CTAB molecules available to enable SWCNT-dispersion reduces. This causes the strong lateral van der Waals attraction between the nanotubes (Han, *et al* 2009) to attract the SWCNTs together to form bundles, as shown in the top phase in Figure 20(b). Therefore this could also be the evidence of the wrapping of carbon nanotubes by polymer chain.

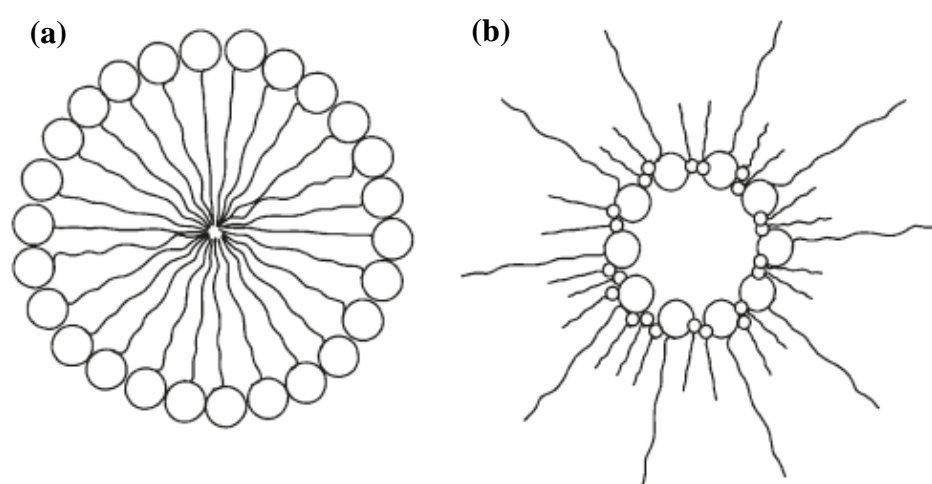


Figure 23 Schematic representation of (a) a CTAB micelle, and (b) a reverse micelle (Gaidamauskas, *et al* 2010)

4.11 Mechanism

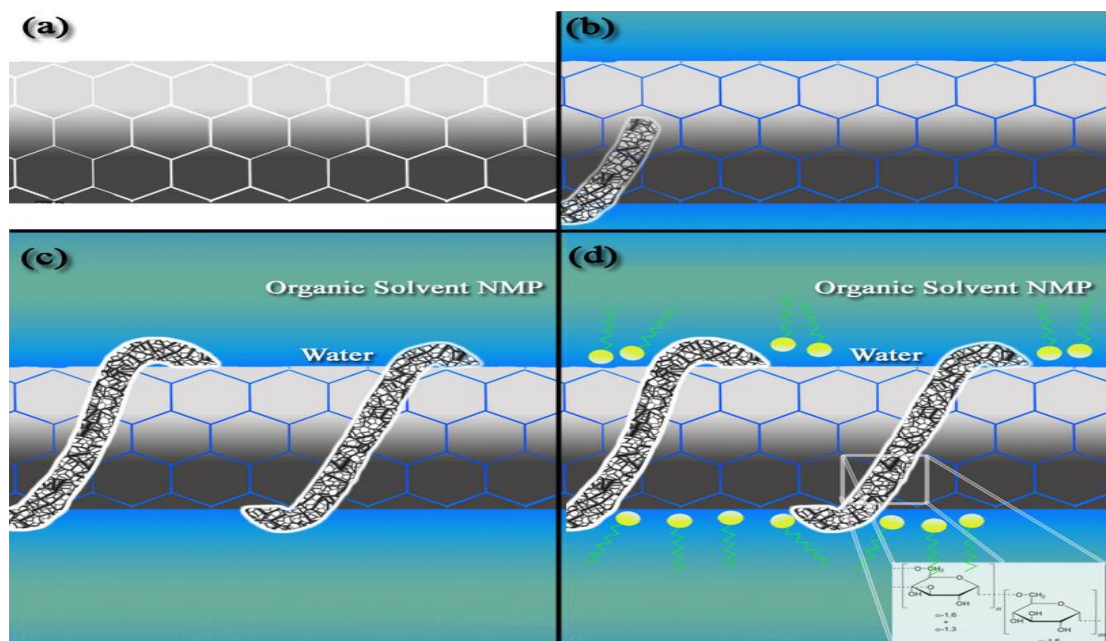


Figure 24 Schematic formation mechanism of polymer around carbon nanotube sidewall in a sequence of (a), (b), (c), and (d)

A plausible mechanism for the separation of the two species of tubes is illustrated in Figure 24. This mechanism is derived according to the evidence collected from the analysis as well as reported intrinsic characteristics of carbon nanotubes. The affinity of amine for semiconducting SWCNTs, for instance, has been reported by numerous authors (Chattopadhyay, *et al* 2003; Feng, *et al* 2011; Furtado, *et al* 2004; Hong, *et al* 2011; Rubianes and Rivas 2007). The AFM results shown in Figure 21 provide possible evidence on the wrapping of polymer around a SWCNT based on works published by Kumar *et al* (Kumar, *et al* 2012). The FTIR results indicate that CTAB is present in the dextran-dominant bottom phase. UV-Vis and Micro-Raman results show that S-SWCNT is more abundant in the dextran-CTAB phase.

Theoretical modelling suggested that the hydrophobic D-glucose units of dextran wrapped around the hydrophobic outer surface of a SWCNT with the hydroxyl

group pointing away from the surface of the SWCNT (Stobinski, *et al* 2008). In our case, the hydroxyl groups of D-glucose attract a thin layer of water in close proximity to the SWCNT outer side-wall. The cationic surfactant CTAB has a polar head and a hydrophobic tail. But CTAB does not dissolved in NMP, which is evenly distributed in both phases. Hence, CTAB molecules selectively embed their polar heads into the thin water layer surrounding the S-SWCNTs with their hydrophobic tails pointing towards NMP-rich environment. Therefore when dextran molecules migrate to the bottom phase, they carry together with them the CTAB molecules, which selectively attach itself to S-SWCNT due to the affinity of S-SWCNT with CTAB's amine group.

Such supramolecular self-organization of surfactant along a tube is called reverse micellar effect as illustrated in Figure 24. This is phenomenon is commonly seen in the purification of enzymes in organic solvents.

4.12 Effect of time, temperature and viscosity of ATPS

Due to the large percentage (up to 42.5% (w/w)) of organic solvent in the system, this ATPS is very different compared to the conventional ATPS. Observations show that the system could not maintain the two phases over a long period of time. The bottom phase would often salt-out if left to incubate for more than 4 hours, whereby it would harden into solid that could not be re-solubilized in water or organic solvent. The nature of the solid has yet to be determined because of its inability to solubilize in water or organic solvent. Therefore it is important to pipette out the top and bottom phase for analysis as soon as two phases are formed.

It is observed throughout the experiment that temperature has a strong influence on the formation of the two phases. It took a longer time for the two phases to form if the ATPS were left to incubate in an oven (45 °C), and relatively shorter time if left to

incubate in the clean room where the temperature is maintained at 19 °C. The two phases will not form, however, beyond a certain threshold temperature (T_T). This threshold temperature is closely related to the concentration of solvents in the system, which is in turn related to the viscosity of each phases of the system. As the temperature increases beyond the T_T , the energy supplied to the polymer molecules by the heat overcomes the intermolecular attraction between polymer molecules. With the extra energy, the molecules are able to move freely. Hence the viscosity of the entire system reduces and the solvent exhibits fluid-like characteristics. The net attractive force exerted by each polymer molecule is weak and therefore unable to form a neat boundary across the system.

As temperature drops, the energy possessed by individual polymer molecule decreases. Therefore the intermolecular attraction becomes dominant and causes the polymer molecules to form long polymer chains. The viscosity increased and the ATPS exhibited gel-like characteristics. The intramolecular attraction of different polymer will give rise to strong surface tension, thus creating a clear boundary. It is observed that as the total concentration of the ATPs increases, the T_T increases as well. This information is crucial because it proves a flexible range of working temperature for ATP.

Nevertheless, it took about 30 minutes for the two phases to form at room temperature. The viscosity of both phases under the influence of temperature has not been quantified in the experiment. However, there is a possibility that the viscosity and temperature of the ATPS will also affect the outcome of the separation (van Berlo, *et al* 1998).

CHAPTER 5: CONCLUSIONS AND FUTURE WORKS

From the results shown in Figure 11, it can be seen that a new ATPS can be formed by using high amount of organic solvent NMP alongside water and polymer. Observation indicates that PEG dissolves readily in NMP, and the resulting phase diagram possesses a similar characteristic as the conventional PEG-water system. Results from the ATPS separation experiment shows that as the molecular weight of PEG increases, the new system becomes more resilient against salt-out.

As for the SWCNT separation experiment, results shows that the best volume ratio for separation of different SWCNT species is 1.5. The UV-VIS diagram in Figure 16 shows the absence of metallic species in the bottom phase. Closer inspection shows the decrement of M-SWCNT in the bottom phase for both volume ratio 1:1 and 1:3. This result is further consolidated by the results from Raman spectroscopy which indicates a broadening of G⁻ band for the bottom phase.

The next step for the experiment is to use the purified carbon nanotubes in the construction of devices such as field effect transistor (FET) and sensor. Nevertheless, we found out that the tubes remain encapsulated within the polymer even after several rounds of washing.



Figure 25 The vacuum filtration system that was used to wash away polymer from the carbon nanotubes

The optical properties of the tubes are not affected as proven by the UV-vis and Raman spectroscopy results. Nevertheless, the presence of polymer around the tubes can significantly disrupt the performance of the device. Theoretically, the polymers are easy to remove due to their hydrophilic nature. However, SEM results show that the polymer molecules remained even after several rounds of washing using deionized water. During the test, the polymer-wrapped nanotubes FET did not allow current to pass through.

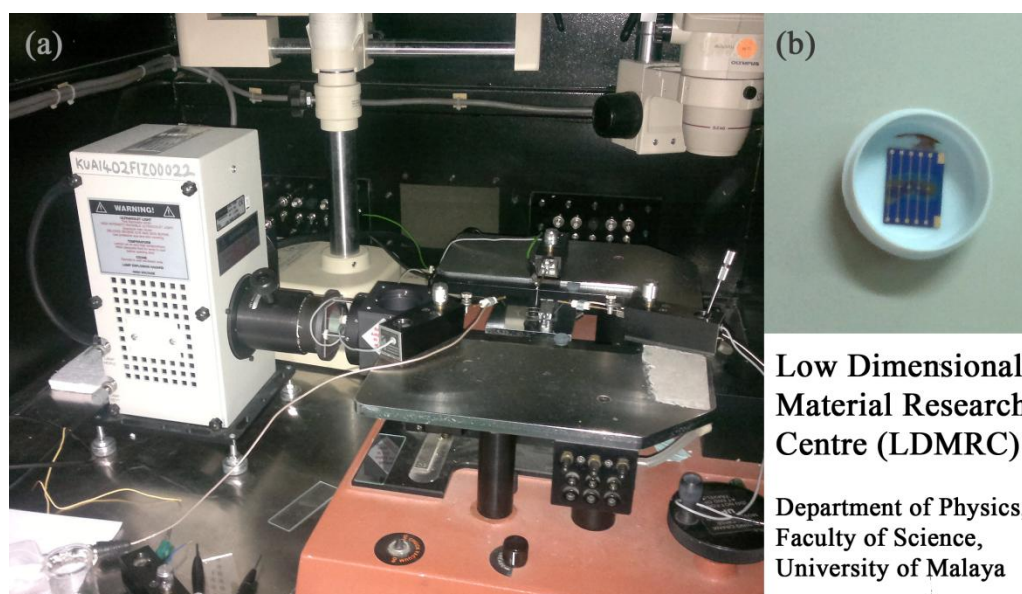


Figure 26 The I-V test of the SWCNT-FET did not yield satisfactory results

This could be due to the intrinsic insulating nature of the polymer preventing the current from reaching and flowing through the tubes. Therefore, it is imperative for any future works to include steps to properly remove the polymers before utilizing the tubes in the construction of devices.

ATPS is a very useful purification technique because it caters not only for a single material but a wide variety of other options. There are so many parameters that can be manipulated to transform the outcome of purification. The most commonly manipulated variable is the type of polymer used for phase separation. Using polymers with the capability of interacting with nanotubes (Feng, *et al* 2011) and forming ATPs (Zafarani-Moattar and Sadeghi 2002) such as polyvinylpyrrolidone (PVP) to replace PEG, or using a combination of both polymers may also yield good results. Other polymers that can be used are Pluronic F108 (Granite, *et al* 2011), Poly(9,9-dioctylfluorenyl-2,7-diyl) (PFO) (Gao and Loi 2010), polystyrene sulfonate (PSS) and Polyethylenimine (PEI) (O'Connell, *et al* 2001).

Apart from that, temperature could also influence the outcome of the purification. It should be noted that ATPS is very sensitive to the changes in

temperature. Different polymers have different characteristics when exposed to different temperature. Some can form ATPS more easily at high temperature, while some form ATPS faster at low temperature. The effect of temperature was not thoroughly studied in this work. Therefore it would be interesting to see how temperature affects the outcome of the purification for SWCNT.

Besides, a combination of cationic and anionic surfactants may also form ATPS. The most famous example for this is the ATPS formed using cetyltrimethylammonium bromide (CTAB) and sodium dodecyl sulfate (SDS) (Wang, *et al* 2011). This method is very interesting because while both of these surfactants are excellent dispersant of SWCNT, CTAB contains amine group while SDS does not. Hence it would be interesting to see the interaction between the semiconducting SWCNT and amine.

ATPS is a famous purification technique in biotechnology, biochemistry and biology-related fields. Therefore it is possible to combine this concept with earlier SWCNT works such as purification of nanotube *via* DNA and aromatic polymer to improve purification results and reduce experimental cost. ATPS has already been used to purify enzymes such as lipase (Show, *et al* 2011; Show, *et al* 2012a; Show, *et al* 2012b), partition human antibodies (Azevedo, *et al* 2009) and in the purification of DNA (Wiendahl, *et al* 2012). It is therefore plausible to combine the earlier work of DNA-carbon nanotubes-purification (Tu, *et al* 2009; Zheng, *et al* 2003) with ATPS. The results of the purification of SWCNT using DNA shows that certain DNAs show selectivity when it comes to the type of SWCNT they wrap. With this in mind, ATPS can be used to further segregate the DNAs according to specification, and therefore also separate the SWCNT according to its chirality. The primary challenge for this combination is finding a way to reduce the cost of experiment.

This work uses the ATPs which can itself become an efficient standalone carbon nanotubes purification method through further optimization. There is an ongoing debate on the interaction between SWCNT with amine and polymers. A 2005 paper by Maeda et al suggests that M-SWCNT is more strongly adsorbed by amine than S-SWCNT (Maeda, *et al* 2005). The experimental results support the existing hypothesis regarding the interaction of amine and carbon nanotubes. Besides, this work has proven to be cost and time efficient while maintaining the high level of purification. This study has shown that polymer encloses on individual nanotubes as shown in FESEM figures.

The future applications of the ATPS purification technique and SWCNT should not be limited to the examples mentioned above. There are a lot to be done in order to bring carbon nanotubes to the realm of large-scale production to benefit mankind in the future.

REFERENCES

- Agasoster T. 1998. Aqueous two-phase partitioning sample preparation prior to liquid chromatography of hydrophilic drugs in blood. *Journal of Chromatography B* 716(1-2):293-298.
- Akhavan O, Abdolabad M, Abdi Y, Mohajerzadeh S. 2009. Synthesis of titania/carbon nanotube heterojunction arrays for photoinactivation of *E. coli* in visible light irradiation. *Carbon* 47(14):3280-3287.
- Albertsson PA. 1986. Partition of cell particles and macromolecules. New York: Wiley.
- Albertsson PA. 1990a. Separation of Cell Particles and Molecules - a Citation-Classic Commentary on Partition of Cell Particles and Macromolecules by Albertsson, P.A. *Current Contents/Life Sciences* (43):22-22.
- Albertsson PA, Johansson, G. and Tjerneld, F. 1990b. Aqueous two-phase separations. Asenjo JA, editor. New York: Marcel Dekker.
- Ando T, Nakanishi T. 1998. Impurity scattering in carbon nanotubes - Absence of back scattering. *Journal of the Physical Society of Japan* 67(5):1704-1713.
- Ando YI, Sumio. 1993. Preparation of Carbon Nanotubes by Arc-Discharge Evaporation. *Japanese Journal of Applied Physics* 32(Part 2, No. 1A/B):2.
- Antov M, Pericin DM, Pejin SN. 2004. Pectinases partitioning in aqueous two-phase systems: an integration of the systems poly(ethylene glycol)/crude dextran and poly(ethylene glycol)/ammonium sulphate. *Journal of the Serbian Chemical Society* 69(4):299-307.
- Arun AK. 2008. European Monoclonal Antibodies Market—How is the Future: Frost and Sullivan.
- Ashipala OK, He Q. 2008. Optimization of fibrinolytic enzyme production by *Bacillus subtilis* DC-2 in aqueous two-phase system (poly-ethylene glycol 4000 and sodium sulfate). *Bioresource Technology* 99(10):4112-4119.

- Attal S, Thiruvengadathan R, Regev O. 2006. Determination of the concentration of single-walled carbon nanotubes in aqueous dispersions using UV-visible absorption spectroscopy. *Analytical Chemistry* 78(23):8098-8104.
- Azevedo AM, Gomes AG, Rosa PAJ, Ferreira IF, Pisco AMMO, Aires-Barros MR. 2009. Partitioning of human antibodies in polyethylene glycol-sodium citrate aqueous two-phase systems. *Separation and Purification Technology* 65(1):14-21.
- Benavides J, Rito-Palomares M. 2008. Practical experiences from the development of aqueous two-phase processes for the recovery of high value biological products. *Journal of Chemical Technology and Biotechnology* 83(2):133-142.
- Benedict LX, Louie SG, Cohen ML. 1995. Static Polarizabilities of Single-Wall Carbon Nanotubes. *Physical Review B* 52(11):8541-8549.
- Bethune DS, Kiang CH, Devries MS, Gorman G, Savoy R, Vazquez J, Beyers R. 1993. Cobalt-Catalyzed Growth of Carbon Nanotubes with Single-Atomic-Layerwalls. *Nature* 363(6430):605-607.
- Bi PY, Dong HR, Yuan YC. 2010. Application of aqueous two-phase flotation in the separation and concentration of puerarin from *Puerariae* extract. *Separation and Purification Technology* 75(3):402-406.
- Bronikowski MJ, Willis PA, Colbert DT, Smith KA, Smalley RE. 2001. Gas-phase production of carbon single-walled nanotubes from carbon monoxide via the HiPco process: A parametric study. *Journal of Vacuum Science & Technology A* 19(4):1800-1805.
- Chattopadhyay D, Galeska L, Papadimitrakopoulos F. 2003. A route for bulk separation of semiconducting from metallic single-wall carbon nanotubes. *Journal of the American Chemical Society* 125(11):3370-3375.

da Silva CAS, Coimbra JSR, Rojas EEG, Teixeira JAC. 2009. Partitioning of glycomacropeptide in aqueous two-phase systems. *Process Biochemistry* 44(11):1213-1216.

da Silva LHM, Coimbra JSR, Meirelles AJD. 1997. Equilibrium phase behavior of poly(ethylene glycol) plus potassium phosphate plus water two-phase systems at various pH and temperatures. *Journal of Chemical and Engineering Data* 42(2):398-401.

Deng J, Ghosh K, Wong HSP. 2007. Modeling carbon nanotube sensors. *IEEE Sensors Journal* 7(9-10):1356-1357.

Dresselhaus MS, Dresselhaus G, Jorio A, Souza AG, Saito R. 2002. Raman spectroscopy on isolated single wall carbon nanotubes. *Carbon* 40(12):2043-2061.

Dresselhaus MS, Saito R, Jorio A. 2005. Semiconducting carbon nanotubes. *Physics of Semiconductors, Pts A and B* 772:25-31.

Durkop T, Getty SA, Cobas E, Fuhrer MS. 2004. Extraordinary mobility in semiconducting carbon nanotubes. *Nano Letters* 4(1):35-39.

Eftekhari A, Jafarkhani P, Moztarzadeh F. 2006. High-yield synthesis of carbon nanotubes using a water-soluble catalyst support in catalytic chemical vapor deposition. *Carbon* 44(7):1343-1345.

Elliott VL, Edge GT, Phelan MM, Lian LY, Webster R, Finn RF, Park BK, Kitteringham NR. 2012. Evidence for Metabolic Cleavage of a PEGylated Protein in Vivo Using Multiple Analytical Methodologies. *Molecular Pharmaceutics* 9(5):1291-1301.

Feng JL, Alam SM, Yan LY, Li CM, Judeh Z, Chen YA, Li LJ, Lim KH, Chan-Park MB. 2011. Sorting of Single-Walled Carbon Nanotubes Based on Metallicity by Selective Precipitation with Polyvinylpyrrolidone. *Journal of Physical Chemistry C* 115(13):5199-5206.

- Fogden S, Howard CA, Heenan RK, Skipper NT, Shaffer MSP. 2012. Scalable Method for the Reductive Dissolution, Purification, and Separation of Single-Walled Carbon Nanotubes. *ACS Nano* 6(1):54-62.
- Forciniti D, Hall CK, Kula MR. 1991. Influence of Polymer Molecular-Weight and Temperature on Phase-Composition in Aqueous 2-Phase Systems. *Fluid Phase Equilibria* 61(3):243-262.
- Furtado CA, Kim UJ, Gutierrez HR, Pan L, Dickey EC, Eklund PC. 2004. Debundling and dissolution of single-walled carbon nanotubes in amide solvents. *Journal of the American Chemical Society* 126(19):6095-6105.
- Gaidamauskas E, Cleaver DP, Chatterjee PB, Crans DC. 2010. Effect of Micellar and Reverse Micellar Interface on Solute Location: 2,6-Pyridinedicarboxylate in CTAB Micelles and CTAB and AOT Reverse Micelles. *Langmuir* 26(16):13153-13161.
- Gao J, Loi MA. 2010. Photophysics of polymer-wrapped single-walled carbon nanotubes. *European Physical Journal B* 75(2):121-126.
- Granite M, Radulescu A, Pyckhout-Hintzen W, Cohen Y. 2011. Interactions between Block Copolymers and Single-Walled Carbon Nanotubes in Aqueous Solutions: A Small-Angle Neutron Scattering Study. *Langmuir* 27(2):751-759.
- Guo T, Nikolaev P, Rinzler AG, Tomanek D, Colbert DT, Smalley RE. 1995a. Self-Assembly of Tubular Fullerenes. *Journal of Physical Chemistry* 99(27):10694-10697.
- Guo T, Nikolaev P, Thess A, Colbert DT, Smalley RE. 1995b. Catalytic Growth of Single-Walled Nanotubes by Laser Vaporization. *Chemical Physics Letters* 243(1-2):49-54.
- Gupta R, Bradoo S, Saxena RK. 1999. Aqueous two-phase systems: An attractive technology for downstream processing of biomolecules. *Current Science* 77(4):520-523.

- Hamon MA, Hu H, Bhowmik P, Niyogi S, Zhao B, Itkis ME, Haddon RC. 2001. End-group and defect analysis of soluble single-walled carbon nanotubes. *Chemical Physics Letters* 347(1-3):8-12.
- Han SW, Oh SJ, Tan LS, Baek JB. 2009. Grafting of 4-(2,4,6-Trimethylphenoxy)benzoyl onto Single-Walled Carbon Nanotubes in Poly(phosphoric acid) *via* Amide Function. *Nanoscale Research Letters* 4(7):766-772.
- Haroz EH, Duque JG, Rice WD, Densmore CG, Kono J, Doorn SK. 2011. Resonant Raman spectroscopy of armchair carbon nanotubes: Absence of broad G(-) feature. *Physical Review B* 84(121403): 1-4
- Hatti-Kaul R. 2000. Aqueous two-phase systems: a general overview. Hatti-Kaul R, editor. Totowa, New Jersey: Humana Press.
- Hirsch A. 2002. Functionalization of single-walled carbon nanotubes. *Angewandte Chemie-International Edition* 41(11):1853-1859.
- Hone J, Whitney M, Piskoti C, Zettl A. 1999. Thermal conductivity of single-walled carbon nanotubes. *Physical Review B* 59(4):R2514-R2516.
- Hong G, Zhou M, Zhang ROX, Hou SM, Choi W, Woo YS, Choi JY, Liu ZF, Zhang J. 2011. Separation of Metallic and Semiconducting Single-Walled Carbon Nanotube Arrays by "Scotch Tape". *Angewandte Chemie-International Edition* 50(30):6819-6823.
- Hong S, Myung S. 2007. Nanotube electronics - A flexible approach to mobility. *Nature Nanotechnology* 2(4):207-208.
- Hustedt H, Kroner K, and Kula M, 1985. Applications of phase partitioning in biotechnology. Walter H, Brooks, D, Fisher, D, editor. Orlando, Florida: Academic Press.
- Iijima S. 1991. Helical Microtubules of Graphitic Carbon. *Nature* 354(6348):56-58.
- Iijima S, Ichihashi T. 1993. Single-Shell Carbon Nanotubes of 1-nm Diameter, *Nature* 364(6439):737-737.

- Jakubek LM, Marangoudakis S, Raingo J, Liu XY, Lipscombe D, Hurt RH. 2009. The inhibition of neuronal calcium ion channels by trace levels of yttrium released from carbon nanotubes. *Biomaterials* 30(31):6351-6357.
- Jimenez D, Cartoixa X, Miranda E, Sune J, Chaves FA, Roche S. 2007. A simple drain current model for Schottky-barrier carbon nanotube field effect transistors, *Nanotechnology* 18(41).
- Jorio A, Santos AP, Ribeiro HB, et al. 2005. Quantifying carbon-nanotube species with resonance Raman scattering. *Physical Review B* 72(7): 1-5
- Joseyacamán M, Mikiyoshida M, Rendon L, Santiesteban JG. 1993. Catalytic Growth of Carbon Microtubules with Fullerene Structure, *Applied Physics Letters* 62(6):657-659.
- Kataura H, Kumazawa Y, Maniwa Y, Umezu I, Suzuki S, Ohtsuka Y, Achiba Y. 1999. Optical properties of single-wall carbon nanotubes. *Synthetic Metals* 103(1-3):2555-2558.
- Kong J, Dai HJ. 2001. Full and modulated chemical gating of individual carbon nanotubes by organic amine compounds. *Journal of Physical Chemistry B* 105(15):2890-2893.
- Kozinsky B, Marzari N. 2006. Static dielectric properties of carbon nanotubes from first principles. *Physical Review Letters* 96(16).
- Krupke R, Hennrich F, von Lohneysen H, Kappes MM. 2003. Separation of metallic from semiconducting single-walled carbon nanotubes. *Science* 301(5631):344-347.
- Krupke R, Linden S, Rapp M, Hennrich F. 2006. Thin films of metallic carbon nanotubes prepared by dielectrophoresis. *Advanced Materials* 18(11):1468-1470.
- Kukovecz A, Kramberger C, Georgakilas V, Prato M, Kuzmany H. 2002. A detailed Raman study on thin single-wall carbon nanotubes prepared by the HiPCO process. *European Physical Journal B* 28(2):223-230.

- Kumar B, Castro M, Feller JF. 2012. Tailoring the chemo-resistive response of self-assembled polysaccharide-CNT sensors by chain conformation at tunnel junctions. *Carbon* 50(10):3627-3634.
- Kurti J, Zolyomi V, Kertesz M, Sun GY. 2003. The geometry and the radial breathing mode of carbon nanotubes: beyond the ideal behaviour. *New Journal of Physics* 5(125):1-25
- Lee WH, Kim SJ, Lee WJ, Lee JG, Haddon RC, Reucroft PJ. 2001. X-ray photoelectron spectroscopic studies of surface modified single-walled carbon nanotube material. *Applied Surface Science* 181(1-2):121-127.
- Li M, Dong HR. 2010. The investigation on the aqueous two-phase floatation of lincomycin. *Separation and Purification Technology* 73(2):208-212.
- Li ZZ, Wu ZY, Li K. 2009. The high dispersion of DNA-multiwalled carbon nanotubes and their properties. *Analytical Biochemistry* 387(2):267-270.
- Lopes AM, Pessoa A, Rangel-Yagui CD. 2008. Can affinity interactions influence the partitioning of glucose-6-phosphate dehydrogenase in two-phase aqueous micellar systems. *Quimica Nova* 31(5):998-1003.
- Madhusudhan MC, Raghavarao KSMS, Nene S. 2008. Integrated process for extraction and purification of alcohol dehydrogenase from Baker's yeast involving precipitation and aqueous two phase extraction. *Biochemical Engineering Journal* 38(3):414-420.
- Maeda Y, Kimura S, Kanda M, et al. 2005. Large-scale separation of metallic and semiconducting single-walled carbon nanotubes. *Journal of the American Chemical Society* 127(29):10287-10290.
- Marquardt CW, Blatt S, Hennrich F, Lohneysen HV, Krupke R. 2006. Probing dielectrophoretic force fields with metallic carbon nanotubes. *Applied Physics Letters* 89(18):1-3

Mazzola PG, Lopes AM, Hasmann FA, Jozala AF, Penna TCV, Magalhaes PO, Rangel-Yagui CO, Pessoa A. 2008. Liquid-liquid extraction of biomolecules: an overview and update of the main techniques. *Journal of Chemical Technology and Biotechnology* 83(2):143-157.

Miyata Y, Mizuno K, Kataura H. 2011. Purity and Defect Characterization of Single-Wall Carbon Nanotubes Using Raman Spectroscopy. *Journal of Nanomaterials* 2011(786763):1-7.

Monthieux M, Kuznetsov VL. 2006. Who should be given the credit for the discovery of carbon nanotubes? *Carbon* 44(9):1621-1623.

Narendar S, Gupta SS, Gopalakrishnan S. 2012. Wave propagation in single-walled carbon nanotube under longitudinal magnetic field using nonlocal Euler-Bernoulli beam theory. *Applied Mathematical Modelling* 36(9):4529-4538.

O'Connell MJ, Boul P, Ericson LM, Huffman C, Wang YH, Haroz E, Kuper C, Tour J, Ausman KD, Smalley RE. 2001. Reversible water-solubilization of single-walled carbon nanotubes by polymer wrapping. *Chemical Physics Letters* 342(3-4):265-271.

Ooi CW, Tey BT, Hii SL, Ariff A, Wu HS, Lan JCW, Juang RS, Kamal SMM, Ling TC. 2009a. Direct Purification of *Burkholderia Pseudomallei* Lipase from Fermentation Broth Using Aqueous Two-Phase Systems. *Biotechnology and Bioprocess Engineering* 14(6):811-818.

Ooi CW, Tey BT, Hii SL, Mazlina S, Kamal M, Lan JCW, Ariff A, Ling TC. 2009b. Purification of lipase derived from *Burkholderia pseudomallei* with alcohol/salt-based aqueous two-phase systems. *Process Biochemistry* 44(10):1083-1087.

Opaprakasit P, Painter PC, Coleman MM. 2004. Dissolution, swelling properties, and complex formation of clays in NMP/CS₂ mixed solvents. *Abstracts of Papers of the American Chemical Society* 227:U1071-U1071.

- Pereira M, Wu YT, Venancio A, Teixeira J. 2003. Aqueous two-phase extraction using thermo separating polymer: a new system for the separation of endo-polygalacturonase. *Biochemical Engineering Journal* 15(2):131-138.
- Rito-Palomares M. 2004. Practical application of aqueous two-phase partition to process development for the recovery of biological products. *Journal of Chromatography B-Analytical Technologies in the Biomedical and Life Sciences* 807(1):3-11.
- Rosa PAJ, Ferreira IF, Azevedo AM, Aires-Barros MR. 2010. Aqueous two-phase systems: A viable platform in the manufacturing of biopharmaceuticals. *Journal of Chromatography A* 1217(16):2296-2305.
- Rubianes MD, Rivas GA. 2007. Dispersion of multi-wall carbon nanotubes in polyethylenimine: A new alternative for preparing electrochemical sensors. *Electrochemistry Communications* 9(3):480-484.
- Ryu H, Kalblein D, Weitz RT, Ante F, Zschieschang U, Kern K, Schmidt OG, Klauk H. 2010. Logic circuits based on individual semiconducting and metallic carbon-nanotube devices. *Nanotechnology* 21(47):475207-475211.
- Saito Y, Inagaki M, Shinohara H, Nagashima H, Ohkohchi M, Ando Y. 1992. Yield of Fullerenes Generated by Contact Arc Method under He and Ar - Dependence on Gas-Pressure. *Chemical Physics Letters* 200(6):643-648.
- Schindler J, Nothwang HG. 2006. Aqueous polymer two-phase systems: Effective tools for plasma membrane proteomics. *Proteomics* 6(20):5409-5417.
- Shim HC, Song JW, Kwak YK, Kim S, Han CS. 2009. Preferential elimination of metallic single-walled carbon nanotubes using microwave irradiation. *Nanotechnology* 20(6):065707-065712.

- Show PL, Tan CP, Anuar MS, Ariff A, Yusof YA, Chen SK, Ling TC. 2011. Direct recovery of lipase derived from *Burkholderia cepacia* in recycling aqueous two-phase flotation. *Separation and Purification Technology* 80(3):577-584.
- Show PL, Tan CP, Anuar MS, Ariff A, Yusof YA, Chen SK, Ling TC. 2012a. Extractive fermentation for improved production and recovery of lipase derived from *Burkholderia cepacia* using a thermoseparating polymer in aqueous two-phase systems. *Bioresource Technology* 116:226-233.
- Show PL, Tan CP, Anuar MS, Ariff A, Yusof YA, Chen SK, Ling TC. 2012b. Primary recovery of lipase derived from *Burkholderia cenocepacia* strain ST8 and recycling of phase components in an aqueous two-phase system. *Biochemical Engineering Journal* 60:74-80.
- Stobinski L, Polaczek E, Rebilas K, Mazurkiewicz J, Wrzalik R, Lin HM, Tomasik P. 2008. Dextran complexes with single-walled carbon nanotubes. *Polimery* 53(7-8):571-575.
- Strano MS, Doorn SK, Haroz EH, Kittrell C, Hauge RH, Smalley RE. 2003. Assignment of (n, m) Raman and optical features of metallic single-walled carbon nanotubes. *Nano Letters* 3(8):1091-1096.
- Tanaka T, Urabe Y, Nishide D, Kataura H. 2009. Continuous Separation of Metallic and Semiconducting Carbon Nanotubes Using Agarose Gel. *Applied Physics Express* 2(12):125002-125005.
- Tang ZK, Sun HD, Wang J, Chen J, Li G. 1998. Mono-sized single-wall carbon nanotubes formed in channels of AlPO₄-5 single crystal. *Applied Physics Letters* 73(16):2287-2289.
- Tolstoguzov V. 2006. Texturising by phase separation. *Biotechnology Advances* 24(6):626-628.

- Tu XM, Manohar S, Jagota A, Zheng M. 2009. DNA sequence motifs for structure-specific recognition and separation of carbon nanotubes. *Nature* 460(7252):250-253.
- Vazquez E, Georgakilas V, Prato M. 2002. Microwave-assisted purification of HIPCO carbon nanotubes. *Chemical Communications* 20:2308-2309.
- Vazquez E, Prato M. 2009. Carbon Nanotubes and Microwaves: Interactions, Responses, and Applications. *ACS Nano* 3(12):3819-3824.
- Veide A, Lindback T, Enfors SO. 1989. Recovery of Beta-Galactosidase from a Poly (Ethylene-Glycol) Solution by Diafiltration. *Enzyme and Microbial Technology* 11(11):744-751.
- Walter H, 1994. Aqueous two-phase systems. San Diego, California: Academic Press.
- Wang F, Chen T, Shang YH, Liu HL. 2011. Two-phase aqueous systems of cetyltrimethylammonium bromide/sodium dodecyl sulfate with and without polyethylene glycol. *Korean Journal of Chemical Engineering* 28(3):923-926.
- Wang XS, Li QQ, Xie J, Jin Z, Wang JY, Li Y, Jiang KL, Fan SS. 2009. Fabrication of Ultralong and Electrically Uniform Single-Walled Carbon Nanotubes on Clean Substrates. *Nano Letters* 9(9):3137-3141.
- Wang Y, Chen LQ, Li YF, Zhao XJ, Peng L, Huang CZ. 2010. A one-pot strategy for biomimetic synthesis and self-assembly of gold nanoparticles. *Nanotechnology* 21(30): 305601-305606.
- Wiendahl M, Oelmeier SA, Dismer F, Hubbuch J. 2012. High-throughput screening-based selection and scale-up of aqueous two-phase systems for pDNA purification. *Journal of Separation Science* 35(22):3197-3207.
- Wu CX, Guan LH. 2011. Increasing the semiconducting component in transparent conducting films of single-walled carbon nanotubes. *Carbon* 49(10):3267-3273.
- www.wikipedia.com. 2009. Atomic Force Microscopy. View of cantilever in Atomic Force Microscope (magnification 1000x).

- Xiao JX, Sivers U, Tjerneld F. 2000. Phase behavior and protein partitioning in aqueous two-phase systems of cationic-anionic surfactant mixtures. *Journal of Chromatography B* 743(1-2):327-338.
- Xiao Q, Wang PH, Ji LL, Tan XK, Ouyang LL. 2007. Dispersion of carbon nanotubes in aqueous solution with cationic surfactant CTAB. *Journal of Inorganic Materials* 22(6):1122-1126.
- Yang CM, Park JS, An KH, Lim SC, Seo K, Kim B, Park KA, Han S, Park CY, Lee YH. 2005. Selective removal of metallic single-walled carbon nanotubes with small diameters by using nitric and sulfuric acids. *Journal of Physical Chemistry B* 109(41):19242-19248.
- Yu MF, Lourie O, Dyer MJ, Moloni K, Kelly TF, Ruoff RS. 2000. Strength and breaking mechanism of multiwalled carbon nanotubes under tensile load. *Science* 287(5453):637-640.
- Yudasaka M, Zhang M, Iijima S. 2003. Diameter-selective removal of single-wall carbon nanotubes through light-assisted oxidation. *Chemical Physics Letters* 374(1-2):132-136.
- Zafarani-Moattar MT, Sadeghi R. 2002. Measurement and correlation of liquid-liquid equilibria of the aqueous two-phase system polyvinylpyrrolidone-sodium dihydrogen phosphate. *Fluid Phase Equilibria* 203(1-2):177-191.
- Zaslavsky BY. 1995. Aqueous two-phase partitioning: physical chemistry and bioanalytical applications. New York: Marcel Dekker.
- Zheng M, Jagota A, Semke ED, Diner BA, Mclean RS, Lustig SR, Richardson RE, Tassi NG. 2003. DNA-assisted dispersion and separation of carbon nanotubes. *Nature Materials* 2(5):338-342.

Zhou ZX, Eres G, Jin RY, Subedi A, Mandrus D, Kim EH. 2009. The performance of *in situ* grown Schottky-barrier single wall carbon nanotube field-effect transistors. Nanotechnology 20(8).